The Method of Cataclastic Analysis of Discontinuous Displacements

Yu. L. Rebetsky and A. Yu. Polets

1 Introduction

Studying regularities of the spatial distribution and temporal variations of tectonic stress is one of the most important issues in a number of disciplines of the Earth sciences. In geodynamics, the problem of understanding of the stress state in the Earth's crust and in the lithosphere is associated with the need to explain the mechanism of formation of the tectonic structures of various scale levels. In seismology, this is a problem of studying the formation mechanism of the earthquake source at the afterschock stage and the development of the post seismic relaxation at the aftershock stage. In geology, a stress state helps to establish interrelations of the formation conditions of the complex structures, discontinuous structures (slip faults) and other deformation structures with mineral deposits. In mining and oil production, stress data provide a safe and efficient exploration of natural resources.

The methods of studying the distribution patterns of tectonic stresses in the earth's crust can be divided into methods of mathematical modeling of stress fields and deformations (physical and mathematical modeling) and experimental methods for studying the tectonic stresses in conditions of naturally occurring rocks. The object of our study will be the methods of the study of natural tectonic stresses on the basis of data directly or indirectly characterizing the deformation process of the rock mass.

It should be noted that the main feature of the problem, which solution will be considered below, consists in the determination of scale levels of the studied stresses. It will be about the tectonic stresses with their different averaging scales of the first meters to tens and even hundreds of kilometers. Such range of the scales is defined by the initial data which gives data on the stress state of a local area of a geological massif,

Y. L. Rebetsky (✉)
Tectonophysics, The Schmidt Institute of Physics of the Earth of the Russian Academy of Sciences (IPE RAS), Moscow, Russia
e-mail: reb@ifz.ru

A. Y. Polets (✉)
Seismology, Institute of Marine Geology and Geophysics Far Eastern Branch of the Russian Academy of Sciences (IMGG FEB RAS), Yuzhno-Sakhalinsk, Russia
e-mail: polec84@mail.ru

S. D'Amico (ed.), *Moment Tensor Solutions*, Springer Natural Hazards,
https://doi.org/10.1007/978-3-319-77359-9_6

sedimentary cover rocks, crust and lithosphere. The uniqueness of the considerable problem is precisely that in such a wide range of scales, the analysis of the state of stress of the earth's interior is carried out according to a unified methodology.

Up to the present time, there were two data sources of such multiscale stresses. The first source is geological data on discontinuous shear displacements of the type—the *slickenside of fault* (the development of the methods began with this data). The second source is seismological data on the of earthquake focal mechanisms (earthquake source model–slip fault). After the development of 3D-seismic methods of reservoir geophysics, it allow us to see the massif structure in detail in depth, it is possible to say that the methods of studying tectonic stresses penetrate into the geophysical data sources.

The problem of studying tectonic stresses should be attributed to the junction of two scientific disciplines such as mechanics and geology. On the one hand, this problem requires knowledge in obtaining geological and geophysical data and knowledge of geological and geophysical property data. On the other hand, this problem requires ability to work in terms of mechanics and tensor analysis. It turned out that, the works in the field of study the tectonic stresses made it possible to create specific approaches in the use of stress tensor analysis, which had not previously been applied in classical mechanics and geomechanics.

It is especially noteworthy that such a well-known scientific discipline as geomechanics has never studied the tectonic stresses in such a wide range of scales. Its knowledge area was the mechanical properties at the scale of the samples according to data from laboratory experiments, as well as local data on the stresses in the rock massif obtained through in situ mining (Hydraulic fracturing, strain gauging, well logging, etc.).

The problem of determining the stresses in a natural massif from data on discontinuous displacements is the main inverse problem in tectonophysics. In the methods are being developed, active faults and discontinuities should be considered as a kind of dynamometers, stress tensometers and deformographs, which are generally used in laboratory rock deformation experiments. Thus, the methods for inversion of the tectonic stresses of a megascopic scale are equivalent, in a certain way, to those instruments for studying stresses deformations, which are available to experimenter in the laboratory modeling, but for objects of incommensurably smaller scales.

This chapter presents a Method of Cataclastic Analysis (MCA) of discontinuous displacements for calculation of tectonic stresses and corresponding semi-brittle deformations of rock massif (Rebetsky et al. 2012, 2016; Rebetsky and Tatevossian 2013). This method includes determination of all components of stress tensors and semi-brittle (faulting) strain increments, together with the estimation of strength parameters of brittle rock massif at the scale level, corresponding to the most representative dimension of faults used for the stress inversion. The main accent of this method is made on the difference in the behavior of continuous solid samples and natural massifs, possessing numerous defects, such as, surfaces of decreased strength, in conditions of their deformation.

This method should be considered as the development of the methodology of studying natural tectonic stress fields, which is based on methods of inversion of

principal stress axes orientations and seismotectonic deformations, created in the works by E. Anderson, M. V. Gzovsky, Yu. V. Riznichenko, J. Brune, E. Carey, J. Angelier, O. I. Goustchenko, S. L. Yunga, P. N. Nikolaev, V. V. Stepanov, J. Gephart, V. D. Parfenov, L. M. Rastsvetaev, L. A. Sim, S. I. Sherman, and others; methods of estimation of strength (stress values) of parts of the Earth's crust, developed in the papers by R. Sibson, G. Renelli, D. Murphy, and others; and the results of laboratory testing of rock samples, described in the papers by K. Mogi, J. Byerlee, J. Handin, R. Stesky, F. Rummel, A. N. Stavrogin, and others.

It is proposed to construct an algorithm for calculating stresses and deformations of the megascopic scale, based on the initial data characterizing the fact of displacement along the planes of faults and cracks. At the same time, if the construction of the algorithm for calculating residual deformations requires only formalization of the transition from the dislocation type of deformation to the continuum dislocation, then to calculate the stresses we need to take some physical concepts about the deformation process and the possible character of the relationship between deformations and stresses.

It should be taken into account that the calculation of the stress tensors parameters, in the form stated above, predetermines averaging over a large megascopic volume (hundreds of meters, the first tens of kilometers) and time (hours and days for aftershock sequences, months and years for earthquakes, hundreds or thousands of years using geological data on cracks).

Therefore, at the considered averaging scale level, the determined stresses and deformations are in fact the generalized forces and the generalized residual deformations—integrants of actually existing tectonic stresses and deformations in the rock massif.

2 The Main Principles of the Method of Cataclastic Analysis of Discontinuous Displacements

The method of cataclastic analysis of discontinuous displacements is applicable for the calculation of modern stress and paleostress. In the first case, seismological data on the earthquake focal mechanisms are used, and in the second case—geological data on the spatial orientation of the fault planes and direction of slickenline. These data characterize the discontinuous structure and the structural-kinematic state of the rock massif. Since the main distinguishing feature of the MCA is the universality of the algorithm, going forward, we will use a term "structural kinematic data" (SKD) on faults for all types of data.

Further in the text, we will use references to seismological data and the relationship between the earthquakes parameters and the stress-strain state of the Earth's interior. However, if instead of parameters that determine the orientation of the poles of the earthquake nodal planes we substitute parameters, characterizing normal to the fault

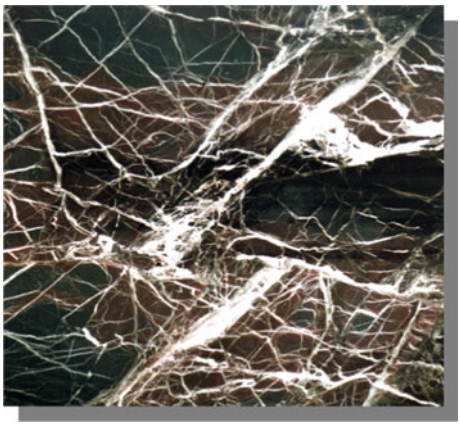

Fig. 1 A natural object showing a large number of closely located existing defects (mineralized cracks)

plane and slickenline vector (rock outcrop), in proper equations, then all the main algorithms of the MCA are stored.

2.1 Model of the Medium and Process of Semi-brittle Deformation

2.1.1 An Elastic Body with a Lot of Slip Faults—The Averaging Scale Is Lower Than the Megascopic

In constructing theory of calculating the stress tensor parameters on the SKD set, we will adopt a model of elastic body, containing a set of intercrossing defects in the form of planes of reduced strength. It is *preexisting faults and cracks* (Fig. 1). This body capable of brittle failure if reached a certain limiting conditions and it is a medium model of the average scale of lower than the megascopic. Stresses of this averaging determine the elastic deformations of the body and formation or activation of faults and cracks.

2.1.2 Dualism of Analysis of the Slip Faults Set

Geo-environment has many different (in scale and in genesis) defects in the form of the differently oriented and intercrossed densely packed in the space of reduced strength surfaces, which are formed primarily by *preexisting faults and cracks*, cleavage, stratification and foliation. During the rock deformation process, the transformation of some elastic deformations into irreversible (residual), causing the mechanical energy dissipation in the corresponding volume of the geo-environment, is carried

out mostly due to shifts along the already existing surfaces of reduced strength (pre-existing faults).

Beginning with a certain averaging scale of time (determined by the number of ruptures) and space (determined by the most representative linear size of the ruptures), the formation of a new or activation of the previously formed slip fault can be regarded as a *faulting deformation* microact (in time). When many microacts united together, they form the process of *faulting flow* of a rock massif. This deforming process is similar to *plasticity flow*. Thus, depending on the scale of averaging, the fault or crack can be considered both as an act of brittle fracture or activation, and as a faulting deformation microact.

2.1.3 The Semi-brittle Body—The Megascopic Averaging Scale

Consideration of a single slip fault as a micro-temporal act of *semi-brittle deformation* for perfectly elastic models is well founded. For such a model, due to the ideal elasticity, every single displacement act along the fault plane is without formation of residual deformations, and it only leads to a redistribution of the elastic deformations and to release of energy. However, displacements along the set of intersecting slip faults lead to fixation of a certain part of the deformations. In this case, residual deformations and internal self-stresses are present, even after all external loading forces have been removed.

Thus, both elastic and residual deformations will present at the appropriate average scale for the chosen model of the geo-environment. Accumulation of these deformation occurs with increasing of intensity of the external loading and involving the number of defects and newly formed cracks in brittle failure. Such geo-environment can be considered as an *semi-brittle body* on a megascopic scale level (Batdorf and Budyansky 1949), and megascopic stresses determine the character of the development of semi-brittle deformations. On a megascopic scale level, such a medium can be considered as an semi-brittle body, and megascopic stresses determine the way of the semi-brittle deformations development.

2.1.4 Newly Formed Slip Faults

It is suggested, that new faults and cracks should cracks in areas for which *brittle strength limit* is exceeded (Fig. 2). According to the principles of fracture mechanics, the planes of newly formed cracks are being formed subparallel to the axis of the intermediate principal stresses. Their normals deviate from the position of the normals of the pair of planes of maximum shear stresses toward the algebraically larger principal stress axis. Respectively, the plane of the slip faults deviates towards the axis of the deviatoric stresses of the maximum compression.

It is obvious that, for natural rock massif, laying of new surfaces of fault take place with involving of already existing areas of reduced strength. Because of this, the strength of the rock massif should be less than the strength of rocks obtained in

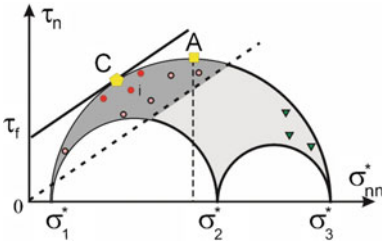

Fig. 2 Mohr diagram and points of stress state for active slip faults (red circles) and active slip faults (green triangles). Yellow pentagon (C) is stress state of new faulting and yellow rectangle (A) is stress state of maximum shear stress plane. Strong line is the brittle strength, broken line is the minimum surface resistance of Coulomb friction (tension stress is positive)

experiments on defect-free samples (Paul 1968; Nikolaevsky 1996). Moreover, this is achieved more by decreasing of the value of internal cohesion of a certain average scale.

2.1.5 Activation of the Preexisting Slip Faults

Since the resistance of inner static friction of already existing, but partially healed faults is less than limiting condition of unbroken areas of the rocks. Therefore, it follows from an analysis of the Mohr diagram that limiting condition of resistance of surface static friction can be overcome for some range of planes orientation of *already existing faults* (Fig. 2). At the same time the planes of active slip faults may deviate in different directions from the plane position defined by the strength limit of internal friction, forming a range of admissible orientation (Rebetskii 2003).

With reasonable certainty it can be assumed that for a certain range of normal stresses acting in the upper part of the tectonosphere, the coefficient of Coulomb friction is close to a constant value (Byerlee 1967). In this case, the limiting condition of Coulomb friction in newly formed faults depends on the normal stress and the ultimate cohesion (limit of strength at zero normal stresses) which can vary from zero (for newly formed faults) to the values of strength limit of the brittle failure for completely healed faults (Byerlee 1978).

2.1.6 Elastic Unloading Area

An *elastic unloading areas* are formed around of each slip faults as a result of the relative movement of its surfaces (planes). The stress state changes significantly within the elastic unloading area. Cumulative inner elastic energy reduced, as a result intensity of the tensor of average deformation and stresses also reduce in the elastic unloading area.

It can be shown that residual deformation which is being accumulated in the geo-environment due to displacement at rupturing (discontinuous residual deformation) corresponds to the value of average elastic deformation relieved in the elastic unloading area (Kostrov and Das 1988). Elastic problem solving for slip faults (Osokina 1988) or anomaly inclusions (Dobrovolsky 2009) shows that the reduction of stresses disturbed by the crack in 10–30 times, at distances of 5–10 lengths of the crack. However, the size of the influence area of the anomaly stress state rises sharply, reaching 50–100 characteristic dimensions of the anomaly, in the case of semi-brittle behavior of the geo-environment (Rebetsky and Lermontova 2016).

2.1.7 Interaction of Closely Located Cracks

At high fracture density, closely located cracks begin to influence on each other after crossing the elastic unloading area of the previously activated crack (Fig. 1). Thus, it is impossible to reject the possibility of mutual influence of the cracks, even in the case of noncrossing cracks. It should be noticed that in a number of previously developed the stress inversion methods was a statement about the possibility of activating a large number of already existing defects of strength in rock massif.

This only explains the observated fact (Angelier 1975; Goustchenko 1975) that the slip faults are formed along planes that deviate from the planes of the maximum shear stresses (or planes with the Coulomb internal friction angle). In methods (J. Angelier and O. Goustchenko) there is an implicit condition: faults do not influence at each other. This condition follows from the principles of the slip theory of plasticity by Batdorf-Budiansky (Batdorf and Budiansky 1949). So, the MCA algorithm assumes *interaction of faults and cracks* in the process of semi-brittle flow.

2.1.8 Initial Sampling of SKD

The condition about the mutual influence of the cracks in the process of semi-brittle flow was instrumental in the MCA algorithm development. This condition actually determined the principle of forming of the calculation of the residual deformations in the overlapping zone of elastic unloading areas of the slip faults—in interaction zone of the cracks. Cracks contribution to the total tensor of residual deformations must be summed up at this particular *area of the cumulative influence of the cracks.* And only this way calculated tensor can be defined as the tensor of generalized residual or semi-brittle deformations.

2.1.9 Steady-State Deformation Process

It is believed that for the steady-state stage of the deformation process, the tensor of increments of semi-brittle deformations tends to become similar to a tensor of elastic deformations at every instant (average scale exceeds the size of the defect-

s—discontinuities, cracks). Such a process of deformation appears for a constant way of applying external and internal loads and uniform rheological properties of a geo-environment, with corresponding average scale (Fig. 3). The tensor of elastic deformations, as well as the stress tensor, is determined by the boundary conditions and the geo-environment properties.

The corresponding tensors of the steady-state stage will be defined as the *short*- and *long*-period components of the stress and deformation tensors (depending on the size of the time averaging). This component of the identified tensors is the main characteristic. Stress tensors and deformation tensors of different averaging scale, with increasing time window and linear averaging scale will converge to this component, with further increase of the loading.

2.1.10 Homogeneous Sample of SKD

The assumption of the regime of steady-state deformation is an essential condition, allowing, in the framework of the MCA, to elaborate the algorithm of finding the parameters of the macrostress tensors and tensors of semi-brittle strains (increments of seismotectonic deformations). It replaces the postulate introduced in Goustchenko's kinematic analysis method—(Goustchenko 1996) and the right dihedral method (Angelier 1984) of the coincidence of the fault plane a slip direction with the shear stress direction, the right dihedral method. This postulate allows for a set of activated in the investigated volume slip faults to select a set of stress states that satisfy the principle of energy dissipation for each faults on the required macrostress tensor.

Thereafter, we will define such states as possible states of stress, and the corresponding sets of SKD as homogeneous samples of the SKD. Thus, a homogeneous sample of SKD determines a set of data on the orientation of the rapture plane and direction of the relative displacement of its sides or on the earthquake focal mech-

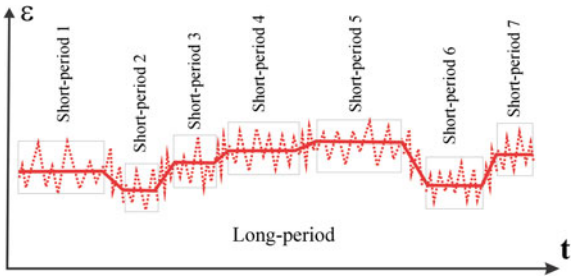

Fig. 3 The difference between the steady state and non-steady state phases of long-period deformation. A straight section of the smooth line shows that the shape of the ellipsoid of full deformations (elastic and irreversible) and its orientation are constant (a *short-period component*). A thin broken line shows the deviations of the ellipsoid of irreversible deformations, which are formed as a result of each act of brittle fracture from the ellipsoid of full deformations (*ultra-short* period component)

anism data that correspond to the conditions of quasi-homogeneity of deformation of the volume where they were fixed for a certain time period. In the MCA, there are criteria that allow one to form a homogeneous sample of SKD by filtering the fractures in the initial sample set.

2.1.11 Tensor of Semi-brittle Deformations for the Faulting Rock Massif

Residual deformation in the rocks can be formed due to cracks and ruptures according to the available data on the level of macro- and mega-scopic deviatoric stresses in the Earth's crust. Actual plastic deformations, occurring as a result of dislocations movement in the crystals and grains, are in the rocks at great depth below Moho (Nikolaevskiy 1996).

Therefore, under the tensor of semi-brittle deformations, we mean the total contribution of discontinuous displacements (averaged over a volume). A dissipation of elastic energy is being occurred within it. In the MCA, the parameters of such a tensor are calculated from data on fractures forming a homogeneous sample of SKD.

2.1.12 Time Variations of the Macrostresses

Essential procedure for calculation of residual deformations is not only spatial averaging, but also time averaging, because the accumulation of residual deformations due to discontinuous displacements occurs over a certain time interval. Thus, within the framework of our study, each point of the geo-environment is a center of four-dimensional volume. In the surrounding activating slip faults areas, the average stress state for unloading volume deviates from the *long-period* component. Thus there is a local change of the stress field in space and time—the *ultrashort disturbance*.

We will define the stress tensor, corresponding to this disturbance, as an *ultrashort* component of the stress tensor. This stress field component of the megascopic averaging scale is the most unstable component in time. Stresses corresponding to this component experience fast (immediately after the rupture displacement), frequent (due to the proximity of the different scale faults) and large changes (because of the difference in the shape of the tensor of external stresses and the tensor of relieved stresses, in consequence of rupture displacement. The deviations of the stress tensor from the long period condition can cover all large areas and act for a relatively long period of time (the first months and years), forming a *short-period* disturbance of the stress field with increasing density of activated and already existed fractures. The stress tensor corresponding to this disturbance condition we will define as *short-period* component of the stress tensor. Activated faults in such time period do not correspond to a long period stress field, and their location and displacement character of their sides are determined by the short period component of the stress tensor.

2.1.13 Influence of the Linear Dimensions of the Slip Faults

The other side of the considerable problem is the linear dimensions of the faults and cracks (the energy level of earthquakes). Stresses and seismotectonic deformations are calculated on the basis of this data. Osokina's studies (1988) show the dependence of the mechanism of small secondary fractures from their linear size, which is due to the hierarchical level of the stress field, responsible for fractures activation of the corresponding length. Therefore, in order to create SKD sample we need criteria that make it possible to determine the quasi-homogeneity of the stress state of different hierarchical levels.

At the same time, the data separation criterion for the scale levels should be not only the linear dimensions of the faults (it is possible such a state for which different linear size of faults will give equivalent results if we use them for the stress inversion), but also the correspondence of their structural-kinematic data to the reconstructed stress tensor. Such criteria exist in the MCA. These criteria are based on the energy limitations of the method.

2.2 Energy Principles of the MCA

2.2.1 Energy Dissipation of an Elastic Deformation

Destruction can occur only when the process of rupture is accompanied by the release of energy. It is follows from the perspective of the semi-brittle deformation of the geo-environment as a result of displacements along a set of slip faults. Upon that, we will assume from the main principles of the plasticity theory that:

- the direction of the average displacement along the single fault coincides with the direction of the vector projection of elastic macrodeformations onto this plane (averaged over the space volume, with a characteristic dimension corresponding to the dimensions of the newly formed fault line) for the tensor that operated here at the time of its appearance- an ultrashort period component;
- displacements along planes of the slip fault set (with regard to the active tensor of elastic macrodeformations and macrostress tensor at this time) may occur arbitrarily for a set of simultaneously activated fractures, but so that a release of mechanical energy occur as a result of such a multiple semi-brittle deformation microact (in time), i.e. the internal elastic energy of the geo environment should decreased. At this time, the total tensor of residual deformations tends to maximally approximate with the tensor of long-period macrodeformations in form and orientation of the principal stress axes. It will provide the maximum efficiency of removing of internal energy.

In considering a series of slip faults activated for a certain time period, it can be said that there is an average tensor of generalized stresses (for this time period). Each act of activation of the fault for this tensor leads to a decrease of internal energy

accumulated in geo environment. This proposition was confirmed experimentally (Bridgman 1949), and it is the main energy principle for development of the MCA algorithm for the tectonic stress inversion.

Further it will be shown that the rule of dissipation of internal elastic energy determines as possible stress states those for which there is an acute angle between the direction of the observed displacement and the vector of shear stress on the fault plane. This relationship can be formalized in the form of inequalities systems.

2.2.2 Note on the Wallace-Bott Hypothesis

The main principles allowing to realize the mathematical formulation of the inverse problem of tectonophysics, within the framework of the dislocations theory, were represented in the studies (Wallace 1951; Bott 1959). It was proposed that average shear stresses τ_n along the plane of fault or crack, acting prior to its activation or formation, coincide in orientation with the direction of the averaging relative displacement $[u_s]$, which is realized in the shift process of the fault side. From this follows the minimal spatial average scale of the study stresses, corresponding to the most representative length of the used faults for reconstruction. It should be noted that this proposition indirectly determines the properties of the geo environment (it corresponds to the isotropic body). The propositions of the R. Wallace and M. Bott can be written in the following form:

$$\tau_n = \sigma_{ns};\ \sigma_{nm} = \tau\left[(1-\mu_\sigma)\,\ell_{n1}\ell_{m1} - (1+\mu_\sigma)\,\ell_{n3}\ell_{m3}\right] = 0. \tag{1}$$

where the ℓ_{ni} and ℓ_{mi} (i = 1, 2, 3) are the direction cosines of the normal vector to the rupture ***n,*** to the shear fracture plane and to the vector ***m*** in the coordinate system *associated with the* principal stresses axes of the source field.

Expression (1) determines that the component of the averaged shear stresses, acting before the slip fault activation, is zero in the shear fracture plane, in the direction of the vector ***m***. This direction is normal to the future direction of the relative displacement of the sides ***s***. Invariants of the stress tensor: the τ (modulus of the maximum shear stresses) and the *Lode-Nadai* coefficient μ_σ or *stress* ratio ($R = (1-\mu_\sigma)/2$), which *characterizes* the *shape* of the *stress ellipsoid*) are related to the principal stresses (uniaxial compression—pure shear—uniaxial tension):

$$\tau = \frac{1}{2}(\sigma_1 - \sigma_3);\quad \mu_\sigma = 2\frac{\sigma_2 - \sigma_3}{\sigma_1 - \sigma_3} - 1,\ \sigma_1 \geq \sigma_2 \geq \sigma_3, \tag{2}$$

where the σ_i ($i = 1, 2, 3$) are the principal stresses. Hereinafter, we will use the concepts of classical mechanics. In the frame of the classical mechanics the compressive stress is negative, and the tensile stress is positive. This is different from the concepts used in mining, where the compressive stress is positive.

In contrast to the assumption made in (Bott 1959; Wallace 1951), it is assumed in the MCA that the direction of the average displacement along the cleavage plane

(vector s) may not coincide with the direction of the tangential stress (vector t) of the sought stress tensor (Fig. 4).

In contrast to the proposition of the R. Wallace and M. Bott, in the MCA, it is considered that the direction of the average displacement along the fault plane (vector s) may not coincide with the direction of the shear stresses (vector t) of the unknown stress tensor (Fig. 4).

The direction of the average displacement **s** must coincide with the direction of the macrodeformation of the elastic shear along this plane for the tensor which existed in the corresponding volume just prior to the slip fault activation—the ultra-short period component of the tensor according to the principles of the MCA. At the same time, the short-period component of the stress tensor and tensor of deformation is unknown.

2.2.3 The Principle of Maximum Dissipation of Internal Elastic Energy for the Unknown Stress Tensor

Formulated above energy dissipation principles for each slip fault, from a homogeneous sample set of SKD, allow one to select noncontroversial possible stress states. In the MCA, the calculation of the stress tensor parameters and increments of seismotectonic deformations is carried out independently on the same set of data. Meanwhile, there are equations for calculation the parameters of the tensor increments for seismotectonic deformations. The equations calculate these parameters on the strength of SKD. Also there are inequations for calculation the stress tensor parameters. These inequalities limit the stress tensor arbitrary. Basically, arbitrary orientations of the principal stress axes can be reduced to a certain predetermined minimum for a large number of data.

MCA uses principle which is in some ways, similar to the well-known in the theory of plasticity *von Mises's principle of maximum plastic dissipation.* In MCA, it is applied to *agreement the* determined parameters of the tensors increments for seismotectonic deformations, stress tensors and to find the only one of all possible states

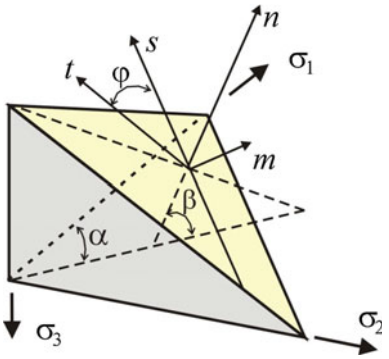

Fig. 4 The mismatch of the displacement vector (***s***) along the fault (***n***—pole of the fault) and direction of the shear stresses (***t***) on the slip fault plane ($\mathbf{m} = \mathbf{n} \times \mathbf{t}$). α, β, φ—azimuth, inclination of the pole of the fault and the displacement angle from strike of the fault

of stress. It is expected that maximum energy dissipation rate of elastic macrodeformations for a homogeneous sample set of SKD is achieved on the tensor of the unknown macrostresses. In accordance with the principle of dissipation positivity, from all possible state of stress permitted for the homogeneous sample set of SKD, in the capacity of unknown state of stress is determined such a state for which the SKD sample set delivers the maximum release of internal elastic energy.

3 The Homogeneous SKD Sample and the Tensor Increments for Seismotectonic Deformation

In the MCA, the problem of calculating the components of the increment tensors of seismotectonic deformations and macro-stresses, as well as the formation of a homogeneous sample of SKD are interrelated tasks that are solved in parallel during the reconstruction. The specific calculating features of the components of the increment tensor for seismotectonic deformations are given on the assumption that for each fault are realized the requirements of energy principles. The formalization principles will be given in the next paragraph. Thus, in fact, it is considered that a homogeneous sample of SKD already exists.

3.1 The Criteria for Creating Homogeneous SKD Sample

Using a model of an initial fracture ideally elastic body as a model of geo environment at the micro-scale level leads to the fact that the model of geo environment with accumulation of residual deformations is obtained (i.e. semi-brittle or cataclastic body) at the macro-scale level of averaging. That is why we will use the fundamental principles of the theory of plasticity during development of the principles of forming *homogeneous samples* set of SKD. Within the framework of the theory of plasticity, there are principles for interconnection between the components of the stress tensors, tensors of deformations and their increments. Calculation of the stress tensor components and increments of seismotectonic deformations should be carried out on the basis of homogeneous sample (set of slip faults or earthquake focal mechanisms). Its formation in the MCA is preceded by the creation of an *initial sample* of SKD. For geological data, this problem is solved by the geologist, at the initial stage of the research, during forming a sample of SKD on the basis of the morphological view of the structures in the rock outcrop. In the case of reconstruction of the modern tectonic stresses on the basis of seismological catalogs of earthquake focal mechanisms, this problem should be solved in the process of calculation on the basis of analysis of geological and tectonic maps or with the involvement of physical laws that allow one to estimate the possible compatibility of the activity of mechanisms included in the SKD sample set.

However, the initial sample of SKD, which is formed on the basis of spatial location of the events and their energy capacity (magnitude) can not yet be considered as a homogeneous sample of SKD, which characterizing the homogeneous deformation phase of the investigated volume. Formation of the homogeneous sample of SKD is the priority issue in the MCA. It should be solved before the reconstruction of stresses and deformations. Criteria that allow one to select data from the initial sample set into the homogeneous sample of SKD are constructed on the basis of energy principles of the theory of plasticity.

3.1.1 Drucker's Postulate

Postulate of positiv work of the actual stress on the increments of plastic deformations is realized for an semi-brittle body with an associated flow law:

$$\sigma_{ij} d\varepsilon_{ij}^{p} \geq 0. \tag{3}$$

An acute angle between the stress vector and the vector of the plastic deformation increments corresponds to this postulate in the six-dimensional stress space. Expression (3) is also one of the consequences of the Drucker's postulate (Drucker 1959), which requires that additional stresses produce non-negative work during a loading process (material stability), for a complete cycle of additional loading and unloading, additional stresses do positive work if plastic strains occur, and zero when the strains are purely elastic.

It should be noted that here and below the positive sign of the normal (principal) stresses corresponds to the extension. Similarly, the positive sign of longitudinal deformations or their increments corresponds to the deformation of elongation. This positive-negative sign convention is accepted in classical mechanics. This is the opposite of the criterion used in mining.

Extend this postulate of positive work (3) of the unknown stresses for each microact (in time) of the semi-brittle deformation, i.e. for each event with the α number from the initial SKD sample set, we can write:

$$\sigma_{ij} d\varepsilon_{ij}^{\alpha} \geq 0. \tag{4}$$

3.1.2 Corollary of the Elastic Energy Dissipation Requirement for Each Slip Fault

Inequality (4) can be rewritten in the coordinate axes associated with the principal axes of the stress tensor (σ_i, $i = 1, 2, 3$). Using representations of the principal stresses through invariants of the stress tensor

$$\begin{aligned} &\sigma_1 = -p + \tau\,(1 - \mu_\sigma/3)\,,\ \sigma_2 = -p + 2\tau\mu_\sigma/3, \\ &\sigma_3 = -p - \tau\,(1 + \mu_\sigma/3) \text{ for } p = -\,(\sigma_1 + \sigma_2 + \sigma_3)\,/3 \end{aligned} \tag{5}$$

and the condition ($d\varepsilon_{ij}^{\alpha} = 0$) of incompressibility at the stage of plastic flow, instead of (4), we will get:

$$\left[(1 - \mu_\sigma)\, d\varepsilon_{11}^{\alpha} - (1 + \mu_\sigma)\, d\varepsilon_{33}^{\alpha}\right] \tau \geq 0. \tag{6}$$

Here $d\varepsilon_{11}^{\alpha}$ and $d\varepsilon_{33}^{\alpha}$ are the increments of longitudinal deformations caused by discontinuous displacement, in the direction of the principal stresses σ_1 and σ_3, respectively. In formula (6), p—is an isotropic pressure.

Since, $\tau > 0$ and the value of the Lode-Nadai coefficient is $-1 \leq \mu_\sigma \leq 1$, then (6) is satisfied for any previously unknown values μ_σ when

$$d\varepsilon_{11}^{\alpha} \geq 0, \quad d\varepsilon_{33}^{\alpha} \leq 0. \tag{7}$$

For a wide class of materials, inequalities (7) determine the range of the possible values of the components of the increment tensor of plastic deformations which formed in the direction of the principal stress axes and satisfying the principle of the internal dissipation elastic energy.

The contribution from each slip fault for the increment tensor of seismotectonic deformation should be an elongation deformation, in the direction of action of the axis of maximum deviatoric tension, and deformation of shortening in the direction of action of the axis of maximum deviatoric compression, according to (7).

We pass from (7) to the inequalities, using earthquake focal mechanism data or data on the planes of the faults and the directions of the slip

$$\ell_{\mathrm{n}1}^{\alpha} \ell_{\mathrm{s}1}^{\alpha} \geq 0, \quad \ell_{\mathrm{n}3}^{\alpha} \ell_{\mathrm{s}3}^{\alpha} \leq 0. \tag{8}$$

Here the direction cosines of the normal vectors to the fault ℓ_{ni}^{α} and slip along it ℓ_{si}^{α} (the cosines of the corresponding angles which determine the position of the poles n and s of the nodal planes of the earthquake focal mechanisms) are also recorded in the coordinate system associated with the orientation of the principal axes σ_1 and σ_3 of the unknown macro-stress tensor.

The inequality (8) determines the geometric locus of points on opposite quadrants, formed by the nodal planes on the lower or upper hemispheres of the earthquake focal mechanism, as an permissible orientation of the axes of the algebraically maximum σ_1 and minimum σ_3 principal stresses. The σ_3 axis should be in the quadrant of P-axis of focal mechanism, and the σ_1 axis should be in the quadrant T-axis of the focal mechanism (Fig. 5).

In the case, when the centroid-moment-tensor (CMT) data are used for reconstruction of the principal stresses the restriction on the possible orientation of unknown stress axes should be determined from the inequalities:

$$dm_{11}^{\alpha} \geq 0, \quad dm_{33}^{\alpha} \leq 0, \tag{9}$$

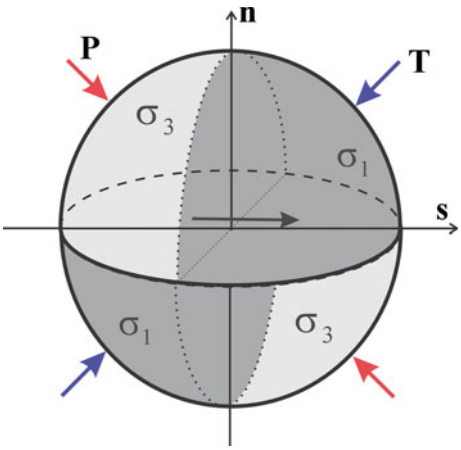

Fig. 5 Areas of possibility orientation principal axes σ_1 and σ_3 for one earthquake focal mechanism. *P* and *T*—axis of focal mechanism of earthquake, *n, s*—poles of nodal planes

where dm_{ii}^{α} $(i=1, 3)$ are the centroid moment tensor components of the earthquake with the index α in the coordinate system associated with the direction of the principal axes of the unknown macrostresses.

The inequalities (7) reflect the relation between the displacements along the fracture surface and change in the energy of the investigated volume. Therefore, we will define inequalities (8) and (9) as the criterion of dissipation elastic energy on each fault in relation to the tensor of unknown macro-stresses.

Inequalities (8) coincide with the well known limitations of the kinematic method (Goustchenko 1996) and the right dihedral method (Angelier 1984). These limitations are obtained as a corollary of the postulate of the coincidence of the shear stress and slip directions. The postulate determines the investigate volume as isotropic, in addition to the requirement that is no mutual influence of the faults of the same scale. Despite the obvious inconsistencies between the postulates of these two methods and the actual state of the geo environment, and the character of semi-brittle deformation process, the results of the stress inversion (on the basis of earthquake focal mechanisms) for the seismically active regions corresponded to the well-known tectonic conceptualization about the current stage of the deformation process in these regions. This analysis showed that the inequalities (8), which are used in the kinematic method and the right dihedral method, have the fundamental roots.

3.1.3 Corollary of the Ordering of Plastic Flow Principle

It will be required the realization of the ordering principle of elastic-plastic deformation (Chernykh 1998) on the unknown macro-stresses tensor, for the contribution to the increment tensor of the seismotectonic deformations from each slip fault:

$$d\varepsilon_{11}^{\alpha} \geq d\varepsilon_{22}^{\alpha} \geq d\varepsilon_{33}^{\alpha}. \tag{10}$$

The inequalities (10) apply more hard restrictions on the deviation of the individual stress contributions to the increment tensor of semi-brittle deformations $d\varepsilon_{ij}^{\alpha}$ from the principal axes orientation of the unknown macro-stresses σ_i $(i = 1, 2, 3)$.

It should be noted that for inequalities (7) and (10), the contribution from each fault to the increment tensor of seismotectonic deformations should provide an elongation deformation in the direction of the axis of the deviatoric stresses of the maximum extension, and a shortening deformation in the direction of maximum deviatoric compression.

From inequality (10) follows an additional limitation: from each slip fault may occur deformation elongation and shortening in the direction of the intermediate principal stress σ_2. In this case, the deformation amplitudes of the elongation should be less than the deformation in the direction of the axis σ_1, and the deformation amplitude of the shortening should be less than the deformation in the direction of the axis σ_3.We will rewrite inequality (10) for the purposes of using data on the earthquakes focal mechanisms or slip faults or centroid-moment-tensor solutions:

$$\ell_{\mathrm{n}1}^{\alpha}\ell_{\mathrm{s}1}^{\alpha} \geq \ell_{\mathrm{n}2}^{\alpha}\ell_{\mathrm{s}2}^{\alpha} \geq \ell_{\mathrm{n}3}^{\alpha}\ell_{\mathrm{s}3}^{\alpha}, \tag{11}$$

$$dm_{11}^{\alpha} \geq dm_{22}^{\alpha} \geq dm_{33}^{\alpha} \text{ for } dm_{11}^{\alpha} + dm_{22}^{\alpha} + dm_{33}^{\alpha} = 0. \tag{12}$$

It should be noted that when (11) and (12) are satisfied the inequalities (8) and (9) are automatically satisfied due to the orthogonality of the vectors $\boldsymbol{s}^{\alpha}$ and $\boldsymbol{n}^{\alpha}$.

Thus, the inequalities (11), (12), that follow from the monotonicity condition of the tensor components of the stresses and deformations apply more hard restrictions on the character of displacements along the fault, relative to the unknown macro-stresses tensor, than the inequalities that follow from the energy dissipation condition. We will define the inequalities (11) and (12) as the criterion of ordering of semi-brittle strain (Rebetsky 1999).

3.2 Cumulative Area of the Elastic Unloading for a Set of Faults

3.2.1 Interaction of the Elastic Unloading Areas of Slip Fault Set and a Criterion of Spatial Proximity of the Faults

The accumulated residual deformations cannot be distributed to arbitrary volumes according to the distribution analysis of the relieved elastic deformations within the old activated or newly created fault. Residual deformations formed as a result of each slip along the fault must be distributed only within the area of elastic unloading of the certain shear.

Thus, the summation of residual deformations should be made only within the mutual intercrossing area of the elastic unloading volumes of many earthquake focal mechanisms, i.e. within the cumulative area. Figure 6 shows the area of elastic

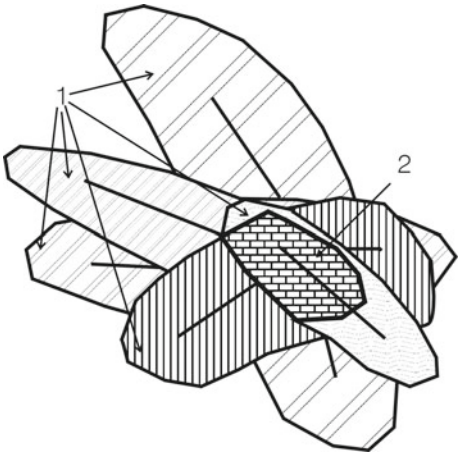

Fig. 6 Calculation of the increment tensor for seismotectonic deformations in the cumulative area (2) of mutual intersection of the elastic unloading (1) areas, which is formed within the earthquakes source areas (faults—black line)

unloading which was formed as a result of several earthquakes in the two-dimensional space. The summation of the deformations, that relieved in the process of earthquakes, is within this area. The above statement is the first criterion of the MCA. It form the basis of the initial sample and then homogeneous sample of SKD. We will define this criterion as criterion of spatial proximity.

It should be noted that, for geological data on discontinuous displacements, the issue of forming the initial sample set is solved by a geologist in the field during collecting data within the a limited geological outcrop. When the geological outcrop is chosen a geologist should analyzed it and indicate the areas of quasi-homogeneous deformation (for example, different limbs of the fold or the fault blocks).

Choosing a geological discovery, the geologist must make his analysis, highlighting the areas of quasi-homogeneous deformation. For example, different fold wings or fracture blocks. In the future, similar preliminary practice of forming the initial sample of SKD will allow one to solve the problem of separating the shifts into homogeneous phases in time. Such a problem is particularly acute for the geological indicators of deformations.

3.2.2 Calculation of the Macro-deformations and Macro-rotation Tensors in the Cumulative Area

It can be written the following formula for the increment tensor of seismotectonic deformations S_{ij} and the rotation tensor π_k for the sample of SKD that is formed in accordance with the criterion of spatial proximity:

$$S_{ij} = \sum_{\alpha=1}^{A} \frac{U^{\alpha}\Omega^{\alpha}}{2\Delta V_{Ue}^{\alpha}} \left(n_i^{\alpha} s_j^{\alpha} + n_j^{\alpha} s_i^{\alpha}\right), \ \pi_k = \sum_{\alpha=1}^{A} \frac{U^{\alpha}\Omega^{\alpha}}{2\Delta V_{Ue}^{\alpha}} \left(n_i^{\alpha} s_j^{\alpha} - n_j^{\alpha} s_i^{\alpha}\right), \ k \neq i, j, \tag{13}$$

where U^{α}—the amplitude of the shear displacement of the rupture sides, Ω^{α}—the square of the rupture, ΔV_{Ue}^{α}—elastic influence zone of the rupture, $n_i^{\alpha} s_j^{\alpha}$ and $n_i^{\alpha} s_j^{\alpha}$—the direction cosines of the poles of two nodal planes of an earthquake source mechanism or the poles to the rupture and the displacement vector along it ($\alpha = 1 \ldots A$—the number of rupture in the homogeneous sample of SKD).

In the MCA it is shown that (13) can be rewritten as:

$$S_{ij} = 0.5 \sum_{\alpha=1}^{A} \gamma_{ns}^{\alpha} \left(n_i^{\alpha} s_j^{\alpha} + n_j^{\alpha} s_i^{\alpha} \right), \ \pi_k = 0.5 \sum_{\alpha=1}^{A} \gamma_{ns}^{\alpha} \left(n_i^{\alpha} s_j^{\alpha} - n_j^{\alpha} s_i^{\alpha} \right), \qquad (14)$$

where γ_{ns}^{α}—the average for the elastic unloading area relieved shear deformation. It is, determined with allowance for correlation of its dimensions and the characteristic dimensions of the earthquake source L^{α} as follows:

$$\gamma_{ns}^{\alpha} = \frac{U^{\alpha} \Omega^{\alpha}}{\Delta V_{Ue}^{\alpha}} \approx 0.01 - 0.1 \frac{U^{\alpha}}{L^{\alpha}}. \qquad (15)$$

Exponential law was determined between the observable values U^{α} and L^{α} in work (Shteynberg 1983). It was done on the basis of processing of a large number of parameters of the various type of earthquakes that occurred in different parts of the Earth. It was found out that the exponent of power is changed in the range from 0.44 to 0.79. A similar analysis was carried out later in the work (Wells and Coppersmith 1994), it allowed to redefine the value of the ratio U^{α}/L^{α}. The value of the ratio U^{α}/L^{α} depends significantly on the type of mechanism realized in the earthquake source. However, in general, relationship between U^{α} and L^{α} is close to linear relationship (the coefficient of the logarithm of the rupture length is about 1) in a double logarithmic coordinate system. It reflects in rather well localized and stretched diagonally cloud of points. At a first approximation, it can be calculated the average value γ_{ns}^{α} (it is approximately about $1–3 \times 10^{-5}$), using the ratio between the maximum sip value and its average value, obtained in works (Starr 1928; Knopoff 1958; Osokina 1988), expression (15) and data from the work (Wells and Coppersmith 1994). This value is much less than the value of the elastic deformations of the strongest rocks.

If we take elastic modulus equal to 5×10^5 bar (50 GPa) than the average relieved stresses can be estimated in the first bars—tens of bars within the elastic unloading area. This value $\gamma_{ns}^{\alpha} = \gamma_{ns} = \tilde{\gamma}$ may be assumed constant and be taken off the sum sign in expressions (14) for the faults from a homogeneous sample set of SKD, characterizing the quasi-homogeneous state of the investigated volume under specific loading conditions. It should be emphasized that the value $\tilde{\gamma}(p, \tau, \mu_{\sigma}, G)$ may differ for neighboring volumes which have same structure and same rheological properties, but different quasi-homogeneous loading conditions. The value $\tilde{\gamma}$, we will define as the geodynamic parameter of the seismotectonic flow.

3.3 The Tensor Increments for Seismotectonic Strains

3.3.1 Normalization of the Tensor

The following formula can be written for *tensor increments of seismotectonic strains* on the basis of (14) and the made above conclusion:

$$\bar{S}_{ij} = I_S \sum_{\alpha=1}^{\mathrm{A}} \left(n_i^\alpha s_j^\alpha + n_j^\alpha s_i^\alpha \right). \tag{16}$$

where I_s is the normalizing factor determined on the basis of the condition $\sqrt{0.5 \bar{S}_{ij} \bar{S}_{ij}} = 1$. Thus, $\bar{S}_{ij}$ is the normalized tensors of increments for seismotectonic strains with the value of the shear intensity equal to 1. For simplicity we will define S_{ij} *as* the tensor of increments for seismotectonic strains, keeping in mind the above mentioned.

3.3.2 Using CMT Solutions

In the case of calculating the tensor increments for seismotectonic strains on the basis of the centroid moment tensor solutions

$$\bar{S}_{ij} = I_S \sum_{\alpha=1}^{\mathrm{A}} \mathrm{m}_{ij}^\alpha, \tag{17}$$

where m_{ij}^a is the centroid moment tensor of the earthquake with the index α. Only four of the six tensor components of the residual macro-deformation can be determined from the results of the reconstruction according to (16) and (17).

This means that three Euler angles that determine the orientation of the principal axes of the tensor and the Lode-Nadai coefficient characterizing the parameters of the deformation ellipsoid will be known after summing the SKD from a homogeneous sample. The value of maximum shift of semi-brittle deformations is characterized by the parameter γ and it remains unknown. This value should be determined on the basis of other data or using additional assumptions.

4 The Calculation of the Stress Tensor (the Principal Stress Axes and the Lode—Nadai Coefficient). The First Stage of the MCA

The possibility of forming a homogeneous sample of SKD, on the basis of the principles following from the theory of elastic-plastic deformation, which adapted

to the analysis of the deformation process of a fractured structure is shown in the previous paragraph. The stress field at the level preceding the considered one is essentially inhomogeneous. That is why in the MCA, the energy principles similar to those that were formulated to forming the homogeneous samples of SKD are used. The concept of generalized stresses for a fractured structure is formulated on the basis of these principles.

4.1 Requirement of Elastic Energy Dissipation—Graphical Algorithm of Realization

It was shown above that inequalities (8) and (9) make it possible to separate the events from the initial sample of SKD, leaving only the events that satisfy to these criteria. The inequalities (8) and (9) was proposed to use directly for determining the position of the principal stress axes in work (Carey and Bruneier 1974; Angelier and Mechler 1977). This approach is based on the limitation for possible orientation of the principal stress axes responsible for the displacement in the earthquake source. This imitation was shown in the work (McKenzie 1969).

The inequality (8) determines the geometric locus of points on opposite quadrants, formed by the nodal planes on the lower or upper hemispheres of the earthquake focal mechanism, as an permissible orientation of the axes of the algebraically maximum σ_1 and minimum σ_3 principal stresses. The σ_3 axis should be in the quadrant of P-axis of focal mechanism, and the σ_1 axis should be in the quadrant T-axis of the focal mechanism. These areas are represented by a corresponding type of hatching (Fig. 7a, b) on the unit lower hemisphere for two different earthquakes.

Thus, the use of only one event from a homogeneous sample makes it possible to halve the range of enumeration for the possible location of the principal stress axes. If two earthquakes are included in homogeneous sample set it is necessary to sum the corresponding quadrants of these earthquake to determine the possible position of the principal stress axes of the tensor (Fig. 7c). Those points on the lower hemisphere, which get into intersection of spatial quadrants of the focal mechanisms are forming a new geometric set. It determines possible location area of exit of the corresponding principal axes (areas: 1 and 2, Fig. 7c). The set of points that get into heteronymous areas are forming a geometric locus where the axes of the principal deviatoric stresses of the maximum compression and tension cannot appear on the hemisphere (area 3 in Fig. 7c).

It should be pointed out that the result of the analysis that was carried out in work (McKenzie 1969) is correct for isotropic medium, i.e. in the case when the principal axes of the tensors of elastic deformations ε_{ij}^{e} and the stress tensor σ_{ij} are coaxial. Dan McKenzie and E. Carey did not to take into account this moment. In fact, in the general case of anisotropic media, the corresponding the principal axes of elastic deformations should be in the quadrants of compression and tension. In the MCA, in the case of steady deformation (tensors ε_{ij}^{e} and $d\varepsilon_{ij}^{p}$ are similar), inequalities (8)

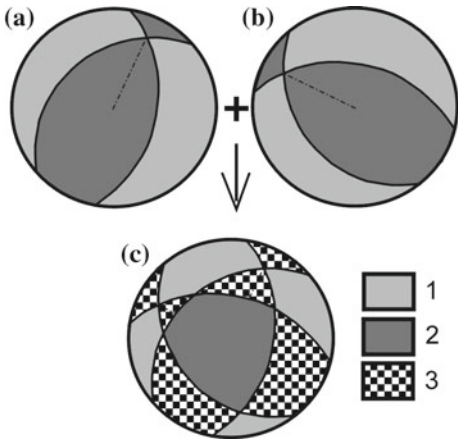

Fig. 7 Summation of the possible location areas of exit of the axes of algebraically maximum and minimum principal stresses on the lower hemisphere according to the inequalities (8): **a**, **b** the quadrants of compression (1) and tension (2) for two different earthquake focal mechanisms, **c** the result of summing the quadrants of compression and tension for two mechanisms. 1—the area of summation only the quadrants of compression, 2—the area of summation only the quadrants of tension, 3—the area of summation the quadrants of compression and tension

and (9) determine distribution of the principal axes of increments for seismotectonic strains S_1 and S_3

The possible exit area of the principal axes of the macrostress tensor to the lower hemisphere can be narrowed by summing the homonym quadrants to relatively small size (the solid angle is less than 15–20°), depending on the number of events in the homogeneous sample of SKD and the variation of their mechanisms (the spread in the orientation of the normal vectors and movements for the fracture share).

Figure 8 shows the final result of the summation of the quadrants of compression and tension for eight events from the initial sample of SKD. One hemisphere determines the possible area of the axes of the maximum deviatoric extension, and the other one the possible area of the axes of maximum deviatoric compression.

Due to the fact that a homogeneous sample set of SKD allow one to calculate the parameters of the increment tensor of seismotectonic strains on the basis of formula (16), the penetration of the principal axes of the tensor S_i ($i = 1, 3$) into the admissible areas on the hemispheres is a validity test of SKD homogeneous sample formation. We will define the areas of mutual intersection of the homonym quadrants as the areas of admissible exit of the principal axes of the increment tensor for seismotectonic strains to the hemispheres.

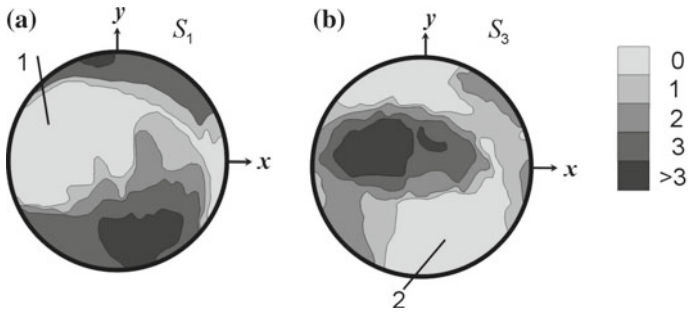

Fig. 8 The result of summation on the lower hemispheres of the quadrants of compression (**a**) and tension (**b**) (see Fig. 7) for finding possibility areas of the principal increments of seismotectonic strains for eight events according to inequalities (8). 1—the possible area of the axis of maximum elongation S_1; 2—the possible area of the axis of the maximum shortening S_3. Shades of gray characterize the numbers of earthquake inconsistent by inequalities (8)

4.2 The Graphic Way of Realizing the Principle of Ordering of Semi-brittle Deformation

The inequalities (11) and (12) make it possible to localize the admissible exit areas of the axes of the tectonic macro-stress tensor in hemispheres in a manner analogous to that considered above. It is important to note the following fact.

The admissible exit areas of algebraically maximum and minimum the principal stresses coincide with the quadrant distribution (as in the case of using inequalities (8), see Fig. 9a, b) for each individual event from a homogeneous sample.

The areas of admissible position of the principal stress axes are marked on the hemispheres according to inequalities (11), will always be inside areas determined by inequalities (8), see Fig. 9, when summing a set of focal mechanisms from a homogeneous sample.

We will define the areas on hemispheres that satisfied inequalities (11) as the areas of admissible exit of the principal stress axes of the macrostress tensor σ_1 and σ_3 to the hemispheres. The localization of the areas of admissible exit of the principal stress axes of the macrostresses to the hemispheres must be carried out on the basis of inequalities (12) if the centroid moment tensor solutions are used for the reconstruction of the state of stress.

4.3 The Determination of the True Orientation of the Principal Axes of the Unknown Stress Tensor

On the one hand, the above mentioned restrictions, on the axes orientation of the unknown tensors of macro-stress and the increments of seismotectonic deformations

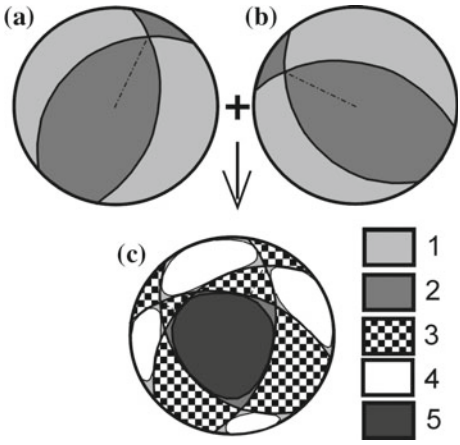

Fig. 9 The summation of the possible exit areas of the axes of algebraically maximum and minimum principal stresses to the lower hemisphere according to the inequalities (11): **a**, **b** the quadrants of compression (1) and tension (2) for two different earthquake focal mechanisms; **c** the result of summation of quadrants for two mechanisms. 1, 2—the areas of summation only the quadrants of compression and extension according to inequalities (8), 3—the areas of summation quadrants of compression and extension according to inequalities (8), 4, 5—the areas inside the quadrants of compression (4) and tension (5) which are satisfied inequalities (11)

with reference to the set of SKD, make it possible to select the range of the possible stress-strain states that best satisfy them. On the other hand, a homogeneous sample of SKD, will characterize the phase of homogeneous deformation of the investigated volume.

Data on the tensor increments for seismotectonic deformations and principle of the maximum dissipation of internal elastic energy, (which is similar to the Von Mises principle in the theory of plasticity), should be used for searching the only possible (correlated) values of the stress tensor.

The Von Mises (Mises 1928) principle determines that, from all possible states, the desired state is that one for which achieved the maximum internal energy dissipation (accumulated in the elastic deformations) on the known tensor of the increments of plastic deformations.

$$\left(\sigma_{ij} - \tilde{\sigma}_{ij}\right) d\varepsilon_{ij}^{p} \geq 0. \tag{18}$$

Where σ_{ij} and $\tilde{\sigma}_{ij}$ are the required (correlated) and possible stress tensors, respectively. By $\tilde{\sigma}_{ij}$ we shall mean the tensor whose axes may have the orientation satisfied by the inequalities (10) or (12) for a homogeneous sample of SKD. We also will use the made above assumption about the similarity of the tensors $d\varepsilon_{ij}^{p}$ and S_{ij}. In this case, the inequality

$$\left(\sigma_{ij} - \tilde{\sigma}_{ij}\right) S_{ij} \geq 0 \tag{19}$$

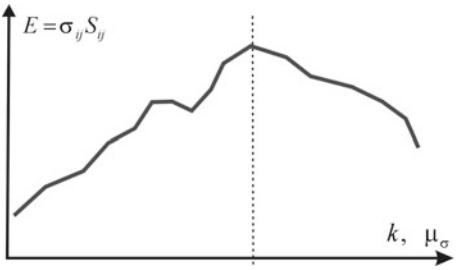

Fig. 10 The scheme is illustrated algorithm of finding a principal stress axis orientation and Lode-Nadai coefficient μ_σ on the base of hypothesis of maximum energy dissipation. k—number of the points on unit half-sphere into areas σ_1 and σ_3 after processing all earthquakes from homogeneous sample

allows us to select the orientation of the principal axes of the macro-stress tensor in the admissible exit areas of the principal stress axes of the maximum deviatoric extension and compression on the hemisphere, and also to select the value of the Lode-Nadai coefficient (it's range of values variations is given by inequality $|\mu_\sigma| \leq 1$).

The inequality (19) determines the maximum for the (in applications to the calculated characteristics of the stress-strain state)

$$E = \sigma_{ij} S_{ij} \tag{20}$$

where

$$\sigma_{ij} = -\left(p - \frac{2}{3}\tau\mu_\sigma\right)\delta_{ij} + \tau\left[(1-\mu_\sigma)\,\ell_{1i}\ell_{1j} - (1+\mu_\sigma)\,\ell_{3i}\ell_{3j}\right], \quad S_{ii} = 0$$

by a discrete search with some step for the Euler angles, (determining the values of the direction cosines ℓ_{ki} ($k = 1, 3$) of the desired principal stress axes in the Cartesian coordinate system), and varying with a small step of values μ_σ from +1 to –1. The search for orientation of the principal axes is carried out within the allocated areas of their possible exit to the corresponding hemispheres (Fig. 10). It is impossible to determine the values of confining pressure and the modulus of the maximum shear stresses according to (19) and (20).

The harmonization of the stress tensors parameters and increments of seismotectonic strains is the main procedure of the MCA. It is carried out after all the events from the initial sample set have been tested for homogeneity or after forming the admissible exit areas of the principal axes of the unknown tensors on the unit hemispheres.

The harmonization is carried out on the basis of the principle of the maximum dissipation of the internal elastic energy, which makes it possible to choose the only one stress state from all possible stress states (the admissible exit areas on the hemispheres determine only possible stress states). Various situations are possible

as a result of using this principle, including those where the calculated tensors of stresses and increments of seismotectonic strains are not coaxial (anisotropy of the medium properties, and the coefficients of the state of the medium are equal (isotropy of the medium properties)).

5 The Calculation of the Relative Values of the Stresses on the Basis of Principles of the Fracture Mechanics. The Second Stage of the MCA

Algorithm for calculating four of the six stress tensor components (orientations of the principal axes of the tensor, determined by the three Euler angles, and the coefficient of the form of the stress tensor or the Lode-Nadai coefficient) was formulated in the previous paragraph.

Two parameters of the stress tensor such as confining pressure and the modulus of the shear stresses remain unknown after the calculations. These parameters are especially important from the point of view of studying geodynamic processes and seismic zoning are unknown. In accordance with the above approach, the obtained results will be interpreted as the results of the first stage of stress analysis.

Nevertheless, in many cases, the field of trajectories of the principal axes of the tensor and the field of the values of the Lode-Nadai coefficient allow one to suggest, with some degree of certainty, the way of external loading of the investigated area of the earth's crust.

These data are extremely important for mathematical or physical modeling, since they make it possible to formulate the boundary conditions of loading. At the same time, the stress tensor parameters, which remain unknown, are the key parameters when estimating the intensity of local loading, the forecast of earthquake preparation areas and areas of increased fracturing. In fact, the values of stresses remain unknown. Algorithm for calculating the relative stress values is presented below. It is based both on the results of laboratory experiments on the destruction of rock samples, and on the fundamental principles of continuum mechanics. Since the calculation of these components is carried out after determining the orientation of the principle axes, the values of the Lode-Nadai coefficient, and also after forming a homogeneous sample set of SKD, the presented calculation algorithm is the second stage of the stress inversion.

In some ways, the proposed approach is based on the intuitive idea that the activation character of the existed fractures should depend on the value of isotropic pressure. At low intensity of all-round compression the range of orientation of newly activated fractures should be greater than for the same set of fractures, but with a higher value of all-round compression.

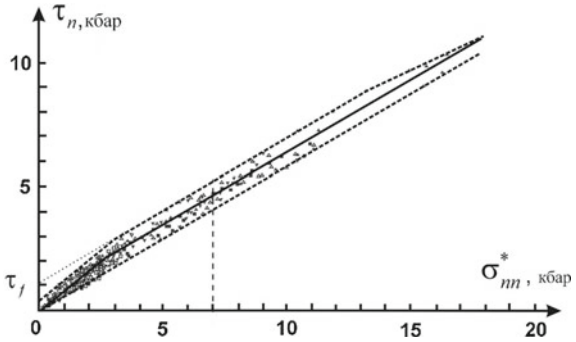

Fig. 11 The results of laboratory experiments on the role of friction in the destruction of rock samples at high pressure (according to Byerlee 1978 with addition dotted lines restricting the cloud of points (experiments): the line of internal strength and line of minimum surface resistance of Coulomb friction)

5.1 Breaking Strength of the Rock and Minimum Frictional Resistance to Ruptures

5.1.1 Experiments on the Destruction of Fractured Rock Samples

The principles for determining the relationship between the spherical and deviator components of the stress tensor are based on the results of brittle failure experiments of rock samples of different types, both initially solid and containing faults or prepared surfaces of reduced strength, performed within the engineering studies (industrial and civil), as well as special geophysical studies (Mogi 1964, 1966; Byerlee 1967, 1968, 1978; Handin 1969; Stesky 1978; Rummel et al. 1978). These experiments made it possible to identify two characteristic lines on the Mohr diagram that determine the breaking strength of internal friction of non-destructive rock samples and the minimum resistance to shear due to friction at the boundaries of already existing faults-(further we will call it the minimum strength friction (Fig. 11).

The indicated lines limit the top and bottom of the main cloud of points (obtained in the experiments) on the parametric area of the Mohr diagram (in the coordinate axes: the normal and shear stresses on the rupture plane) (see Fig. 11). The upper convex line is the limiting envelope. The points obtained in experiments with initially solid samples tend to this line. The lower line determines the states on the rupture sides which correspond to the minimum and zero values of surface cohesion. In a number of experiments it was shown that the line of minimum strength of Coulomb friction comes to the origin of coordinates (Handin 1969; Stesky 1978; Rummel et al. 1978).

It should be noted that Beyrlee's experiments were carried out for the samples under dry conditions, i.e. without the fluid addition. In reality, the fluid pressure

simplify the formation of slip fault in the fractured-pore space of the rocks i.e. the pressure on the shear bands is reduced.

The equations for these lines can be represented in the following form (taking into account the weakening effect of the fluid pressure (Terzaghi 1943):

$$\tau_{Cc} = \tau_n + k_f \sigma^*_{nn} = \tau_f,\ \tau_n + k_s \sigma^*_{nn} = 0 \text{ при } \sigma^*_{nn} = \sigma_{nn} + p_{fl}. \tag{21}$$

Here τ_{Cu}—Coulomb stress determined by the level of the shear stresses (τ_n) and effective (taking into account the fluid pressure) normal stresses (σ^*_{nn}) acting on the plane of the formed or activated fracture. Strength parameters k_f and k_s are the coefficients of internal and surface friction, respectively; and τ_f is the value of internal cohesion or the breaking strength at shear of the intact rock samples. k_f и τ_f are the functions of the σ^*_{nn} in accordance with the results of experiments. This dependence is especially evident at low (less than 3 kbar) and high (more than 15 kbar) values of pressure on the fault plane. The upper limit line gradually flattens out at pressures of more than 20 kbar.

It is important to note that there is an extended area for which the upper bounding line is approximately parallel to the lower line. It can be assumed that $k_f \cong k_s$, $\tau_f \cong$ const for this area. Such an interpretation is possible for a section of the horizontal axis, where the normal pressures on the fracture planes are from 3 to 15 kbar according to the results of experiments.

5.1.2 Minimum Frictional Strength of Existing Faults

This interpretation of the results of the experiments is accepted as a basis of the method for calculating the values of the macro-stress tensor. We will assume that slip along flanks of partially resistive faults is realized with dry friction according to the Coulomb law with a constant value of the surface friction coefficient (k_s = const) for the critical states, (the critical states correspond to the activation process on partially resistive fractures). In addition, the surface cohesion for newly activated faults can vary from the minimum (zero) value to the maximum value that equal to the internal cohesion value of undestroyed massif ($\tau_s \leq \tau_f$). Thus the difference of the limit states lies in the different cohesion values $0 \leq \tau_s^i \leq \tau_f$ for faults with the same value σ^*_{nn} on their flanks.

All possible limit states on the bands of newly formed or activated ruptures can be represented in the following form:

$$\tau_{Cu} = \tau_n + k_s \sigma^*_{nn} = \tau_s^i \text{ when } \quad 0 \leq \tau_s^i \leq \tau_f \text{ и } \sigma^*_{nn} < 0. \tag{22}$$

If the Coulomb stress τ_{Cu} is less than the cohesion τ_s^i for the partially resistive faults, the fault will not activated, although it may lay within the brittle fracture band. But if, the cohesive strength decreases and becomes equal to τ_{Cu} the fault will active.

5.1.3 The Relationship Between the Proposed Approach and the Theory of J. Byerlee

In constructing a theory of failure—determining the stresses responsible for brittle fracture of the rocks, J. Byerlee drew a median line through a cloud of experimental points, averaging the results of observations for initially solid samples, as well as for samples with prepared surfaces of reduced strength and fractures. This approach is applicable for forward modeling to determine the areas of intensive destruction in the Earth's crust. But it is unproductive for the inverse problem, when it is necessary to reconstruct the stress values responsible for the deformation process on the basis of activated fractures data. In this case, the all set of experimental data should be used. It follows that, destruction processes should be characterized by two laws: the limit of internal friction for solid areas of rocks—the Mohr's envelope, and the law of dry friction for already existing but partially resistive faults and fractures—the line of minimum resistance due to friction starts at the origin.

Thus, the medium area of the Mohr diagram (Fig. 9) is taken as the starting point in developing the calculation method. This is the area where both limiting lines are parallel. The strength value τ_s^i may take different values along differently oriented planes of fractures (without exceeding the limit of cohesion value τ_f) according to (22). Probably, the value τ_f may be different for different types of the earth's crust and it should depend on the history of tectonic development of the investigated area and its current structural-tectonic state. In any case, the value τ_f for the rock massif should be less than the value of maximum cohesion obtained from experiment on the destruction of rock samples approximately (1 kbar).

It should be noted that the value of the coefficient of surface friction, acting on the fracture planes in the rock massif, may also differ from the values obtained in the experiments on the samples ($k_s = 0.85$; $k_s = 0.6$).

5.2 *Mohr Circle Diagram and Areas of Admissible Position of Brittle Fractures*

5.2.1 Representation of Stresses on Ruptures on the Mohr Diagram

The possibility of solving the problem, which was formulated at the beginning of this paragraph, will be estimated using the limiting condition (22). To do this, we depict on the Mohr diagram the areas for which slip faults activation is possible with the cohesion variation on their wings $0 \leq \tau_s^i \leq \tau_f$ (i the number of fractures in the homogeneous sample). The size and type of the area of admissible solutions (the permissible orientation of the activated fractures) depend not only on the slope of the limiting lines, (that determine the range of possible conditions on the rupture), but also on the type of the state of stress (the values of the Lode-Nadai coefficient) (Fig. 12).

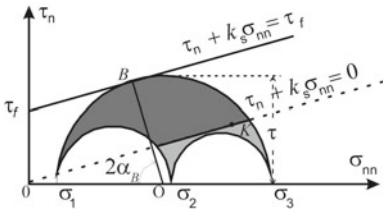

Fig. 12 The Mohr circle diagram and the line of minimum resistance due to friction on existing faults (dotted line) and the line of brittle strength (solid line) for the general case of stress state. Dark grey area is the area of the permissible position of the fractures planes (with cohesion $0 \le \tau_s^i \le \tau_f$). Light gray areas—other areas of possible states at arbitrary planes

It should be pointed out that the center of the Mohr circle (point O, Fig. 12) will correspond to the value of the compressive effective normal stress acting on the areas of maximum shear stresses, which according to the expressions (5) can be represented as:

$$\sigma_O^* = -\left(p^* + \frac{\mu_\sigma}{3}\tau\right) \text{ при } p^* = p - p_{fl}, \tag{23}$$

where p^* is the effective pressure (in this case, the effective pressure is the tectonic pressure minus the pore fluid pressure).

5.2.2 The Uniaxial State of Deviatoric Stresses

We will analyze the Mohr circle diagram (Fig. 12) to estimate the influence of the stress values on the distribution of the fracture planes. This is easier to do for the case when the type of the stress tensor is uniaxial compression or uniaxial tension. In this case, the points characterizing the stresses on inclined surfaces lie on a large Mohr circle. The shear stresses ($\tau_n = \sigma_{nt}$) and normal (σ_{nn}^*) stresses acting on inclined planes ($\boldsymbol{t}$ is the vector determining the direction of action of shear stresses on the plane with the normal in the form of the vector n) are determined according to the expressions:

$$\tau_n = \tau \sin 2\alpha;\ \sigma_{nn}^* = -p^* + \left(\cos 2\alpha - \frac{\mu_\sigma}{3}\right)\tau, \tag{24}$$

where α is the angle between the axis σ_1 and the normal n to the plane of the fracture.

In the case of seismological data, it is believed that the orientation of the rupture plane (we shall return to the issue, how to be determine this plane) and slip direction in the earthquake source area are known. It is in the same way as in the case of reconstruction on the basis of geological shear fracture data. It is also believed that the stresses reached their limiting values (when new formation of ruptures becomes

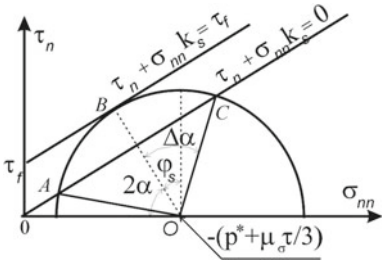

Fig. 13 The Mohr diagram for the case of a uniaxial state of stress. φ_s—the angle of internal and surface friction, $\alpha = \alpha_B$—the angle between the axis of the algebraically maximum principal stress and the pole to the plane of internal friction

possible in the undistracted parts of the rocks), as a result of loading the earth's crust. In this case, the activation of all range of orientations of the fractures, that get into the area between (Fig. 13) the below line of minimum resistance due to friction and the above line of brittle strength (arc AC), becomes possible. Suppose that we have succeeded in fixing the position of the planes of slip faults, which poles of the faults has a minimum and maximum deviation from the direction of the axis of deviatoric compression (points A and C, Fig. 13).

We assume that the actual geo-mechanical characteristics of the rock massif are unknown (i.e. characteristics that satisfy the averaging scale which correspond to the length of the activated ruptures. We will also assume that the orientation of the principal stress axes and the value of the Lode-Nadai coefficient were determined as a result of applying the MCA algorithm to the chosen set of fractures (the first stage of the MCA). The problem consists in calculating the values τ, p^* and in determining the coefficient of surface friction of the geo environment k_s from data on the slope angles of the sip fault planes, in relation to the principal axes of the stress tensor that were reconstructed at the first stage.

According to the above assumption, the line passing through the extreme points A and C on the Mohr diagram (see Fig. 13) should be considered as the line of minimum resistance to dry friction of existing fractures. Using (24), the limiting condition for the frictional resistance for ruptures (22) that correspond to these points can be written in the following form:

$$\tau \sin 2\alpha_i + k_s\left[-p^* + \tau\left(\cos 2\alpha_i - \frac{\mu_\sigma}{3}\right)\right] = 0 \text{ при } i = A,\ C. \tag{25}$$

Whence it follows that

$$\frac{p^*}{\tau} = \frac{\sin 2(\alpha_C - \alpha_A)}{\sin 2\alpha_C - \sin 2\alpha_A} - \frac{\mu_\sigma}{3} \tag{26}$$

by virtue of the fact that

$$2\alpha_A = 2\alpha_B - \Delta\alpha,\ 2\alpha_C = 2\alpha_B + \Delta\alpha \text{ and } \alpha_B = (\alpha_A + \alpha_C)/2. \tag{27}$$

Then the second expression in (33) can be rewritten in a more compact form:

$$\frac{p^*}{\tau} = \frac{\sqrt{1+k_s^2}}{k_s}\left(\cos\Delta\alpha - \frac{\mu_\sigma}{3}\right) \text{ при } k_s = \text{tg } \varphi_s = \text{ctg}2\alpha_B, \tag{28}$$

where $\varphi_s = 90 - 2\alpha_B$—angle of internal friction.

The limit state for point B (the tangency point of the brittle fracture line with the Mohr circle) can be written in the following form:

$$\tau \sin 2\alpha_B + k_s\left[-p^* + \tau\left(\cos 2\alpha_B - \frac{\mu_\sigma}{3}\right)\right] = \tau_f. \tag{29}$$

Point *B* on the Mohr diagram, (in accordance with the assumption of equality of the coefficients of surface and internal friction), corresponds both to the limit of brittle strength for newly created fractures and to the limiting resistance due to friction on already existing faults, the cohesion of which has been restored to the value of internal cohesion τ_f of undistracted areas.

Expression (29), together with (28), makes it possible to determine the value of the invariants of the stress tensor

$$\tau = \frac{\sin 2\alpha_B}{1 - \cos\Delta\alpha}\tau_f, \quad p^* = \frac{\cos\Delta\alpha - \frac{\mu_\sigma}{3}\cos 2\alpha_B}{(1 - \cos\Delta\alpha)\, k_s}\tau_f. \tag{30}$$

Thus, in this case of a uniaxial stress state, the data on the orientation of the two planes of faults (which deviate most strongly from each other) are enough both for determining the coefficients of surface and internal friction of rocks, and for estimating the relative values of maximum shear stresses (up to an unknown value of internal cohesion) and isotropic effective pressure.

5.3 *Determination of Relative Values* p* *and* τ

5.3.1 Reduced Stresses

The calculation algorithm will be constructed for the general case of the state of stress, based on the assumption about possibility of forming faults of arbitrary orientation that formed in accordance with criterion (22). It is considered that the sample set of earthquake focal mechanisms data (faults), (calculation of the principal stress orientation and the Lode-Nadai coefficient are performed on the basis of this sample), is enough representative and it contain the definitions of the faults planes for the all possible range of their orientations within the investigated volume (it also includes fractures with the cohesion value $\tau_s = 0$). The case of reconstruction from seismological data on the earthquake focal mechanisms, when we do not know the actual fault plane will be considered below.

The problem will be formulated in the same way as it was done for the uniaxial state of stress under the assumption that the value of the coefficient of surface friction is known. In this case, a point on the Mohr diagram should be chosen in order to draw the line of minimum resistance. The point (K, Fig. 12) characterizes the state of stress on the surface of one of the faults. The length of the perpendicular that drawn from the center of the circle will be minimal for the point. The values of the stresses on the faults surface can be represented as

$$\sigma_{nn}^{i} = -\left(p + \tau\mu_{\sigma}/3\right) + \tau\tilde{\sigma}_{nn}^{i};\ \tau_{n}^{i} = \tau\tilde{\tau}_{n}^{i}, \tag{31}$$

where $\tilde{\tau}_{n}^{i} = \tilde{\sigma}_{nt}^{i}$ и $\tilde{\sigma}_{nn}^{i}$—the reduced stresses and

$$\tilde{\sigma}_{nj}^{i} = \left(1 - \mu_{\sigma}\right)\ell_{1n}^{i}\ell_{1j}^{i} - \left(1 + \mu_{\sigma}\right)\ell_{3n}^{i}\ell_{3j}^{i} + \delta_{nj}\mu_{\sigma},\ j = n, t, \tag{32}$$

where ℓ_{kn}^{i} and ℓ_{kt}^{i} are the direction cosines of the normal vector $\boldsymbol{n}$ to the fault plane (with the i number from the homogeneous sample), and the vector of the shear stresses $\boldsymbol{t}$ on this plane, in the coordinate system associated with the principal stress axes ($k = 1, 2, 3$). Henceforward, the superscript at stresses identifies the point on the Mohr diagram.

The introduced definition of the reduced stresses is very important, since it allows one to construct Mohr diagrams for the homogeneous samples set of SKD without data on the values of pressure and the maximum shear stress. The diagrams characterize the limiting states on the faults surfaces.

5.3.2 Calculation of the Relative Values of the Effective Pressure and the Maximum Shear Stresses

The ratio of the value of the confining pressure to the modulus of the maximum shear stresses can be determined using expressions (22) and (31). For this purpose, we will assign to a slip fault the minimum possible value of surface cohesion ($\tau_{s}^{K} = 0$), which has a minimum perpendicular length that drawn from the center of the circle (point K, Fig. 12),

$$\frac{p^{*}}{\tau} = \frac{1}{k_{s}}\left(\tilde{\tau}_{n}^{K} + k_{s}\tilde{\sigma}_{nn}^{K}\right) - \mu_{\sigma}/3. \tag{33}$$

The limiting expression (22) is valid for the point B, in which the line of maximum strength of rocks (the limit of internal friction) touches the Mohr circle. The expression (22) is written for the maximum value of cohesion $\tau_{s}^{B} = \tau_{f}$. Using it on the basis of this expression and expressions (31) and (33), we will obtain:

$$\left\langle\frac{\tau}{\tau_{f}}\right\rangle = \frac{1}{\operatorname{cosec}2\alpha_{s} - \left(\tilde{\tau}_{n}^{K} + k_{s}\tilde{\sigma}_{nn}^{K}\right)};\ \left\langle\frac{p^{*}}{\tau_{f}}\right\rangle = \frac{\left(\tilde{\tau}_{n}^{K} + k_{s}\tilde{\sigma}_{nn}^{K}\right) - k_{s}\mu_{\sigma}/3}{k_{s}\left[\operatorname{cosec}2\alpha_{s} - \left(\tilde{\tau}_{n}^{K} + k_{s}\tilde{\sigma}_{nn}^{K}\right)\right]}, \tag{34}$$

where $\alpha_s = \frac{1}{2} \arctan \frac{1}{k_s}$.

Expressions (34) allow one to calculate the relative values of the effective pressure $\langle p^*/\tau_f \rangle$ and the modulus of the maximum shear stresses $\langle \tau/\tau_f \rangle$ on the basis of the results of the first stage of MCA reconstruction and data on the values of the coefficient of surface friction k_s. We will use the angle brackets for the normalized values of the effective pressure and maximum shear stresses.

It should be remembered, that we don't know which of the two nodal planes is the actual fault plane. Within the framework of MCA, there is a criterion for determining the actual fault plane, which directly follows from the Coulomb condition (22). It corresponds to the energy approach that developed in the MCA.

It should be noted that, in the construction of the calculation algorithm, the assumption about the core role of the total value of the shear stress $\tau_n = \sigma_{nt}$ acting on the plane of the activated fault was brought in the calculation algorithm, instead of the shear stress acting in the direction of the slip vector σ_{ns}. It is the total shear stresses acting on the fault plane are responsible for overcoming friction (destruction of the roughness of the bands of the fault, that impede movement).

The deviation of the slip direction along the rupture plane from the shear stress direction may be due to anisotropy in brittle failure zone (the existence of the large roughness besides small one, oriented roughness—fault plane corrugation) or it may be due to the kinematic limitation, caused by rupture structure of the geo environment (cutting by other faults).

5.4 Criteria for Selecting One of the Nodal Planes as the Actual Fault Plane

The knowledge of the orientation of the actual fault plane is a necessary condition for using the expressions (34). Two nodal planes (for double-couple earthquake focal mechanism) represent two variants of position of such a plane in the stress reconstruction from seismological data. There are data on the position of the actual fault planes only for earthquakes, which faults break the surface or for sufficiently large earthquakes. The MCA includes new criteria for selecting one of the nodal planes as the actual fault plane.

5.4.1 Criteria for Selecting the Actual Fault Plane

We will assume that the slip fault corresponds to the nodal plane with the normal $\boldsymbol{n}$ that satisfies the condition:

$$\left(\tilde{\tau}_n^i + k_s \tilde{\sigma}_{nn}^i\right) - \left(\tilde{\tau}_s^i + k_s \tilde{\sigma}_{ss}^i\right) > 0. \tag{35}$$

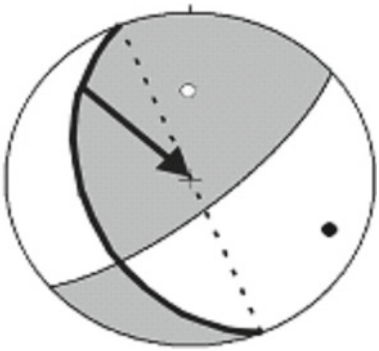

Fig. 14 The double-couple earthquake source mechanism of the 1994 Shikotan earthquake with the selected actual fault plane (in accordance with the criterion (35)) and slip direction (lower hemisphere)

In other words, from two nodal planes of the earthquake focal mechanism, the actual fault plane is that plane for which the Coulomb stresses are greater than for other.

The nodal planes delivering points to the left upper part of the summary Mohr diagram are more preferable as the actual fault plane according to maximumal. Criterion (35) works formally, in the case, when the nodal planes are close to the shear stresses planes, because the points of these nodal planes on the Mohr diagram are located near the vertical axis. In fact, the criterion (35) predetermines that the actual fault plane is that one which has the greater value of cohesion τ_s^i. As will be shown later, this means that the value of the stress drop for the chosen plane will also be greater.

5.4.2 Examples of Using Criteria for Selecting the Actual Fault Plane

For example, the criterion (35) was applied for choosing the actual fault plane for the Shikotan earthquake of 4th October, 1994 (M_b =7.4, the coordinates of the earthquake were—43.71 N, 147.33 E, depth 33 km). The performed calculations, based on catalog data of Global CMT Project (http://www.globalcmt.org), made it possible to monitor the source area before and after the earthquake. These results are presented in Table 1. The best approximation of the CMT solution for the analyzed earthquake determines the position of the poles of two nodal planes with azimuths and dip angles for **n** 68° and 49° and ***s*** 320° and 16°, respectively. The double-couple earthquake source mechanism is shown in Fig. 14.

As can be seen from the data (Table 1), the orientation of the principle axes of the macro stress tensor has stabilized a few years before the catastrophic earthquake (since 1989). The Lode-Nadai coefficient varied from 0.07 to 0.18 for the entire monitoring period and just before the earthquake the Lode-Nadai coefficient was 0.08. The calculations allow us to obtain the values of the reduced stresses for both nodal planes according to expressions (32): $\tilde{\sigma}_{nn} = 0.585$, $\tilde{\sigma}_{ss} = -0.645$, $\tilde{\tau}_n = 0.731$, $\tilde{\tau}_s = 0.764$.

Table 1 The results of stress monitoring for a volume with a center of 43.5° E and 147.5° N

Date	Azimuth σ_1	Dip σ_1	Azimuth σ_3	Dip σ_3
1983.04	316.4	64.8	129.4	22.1
1983.08	345.9	65.2	121.7	17.9
1985.03	316.4	64.8	129.4	22.1
1985.03	315.6	73.1	127.8	16.7
1985.03	304.5	68.5	129.3	21.5
1987.06	345.9	65.2	136.1	21.9
1988.03	345.9	65.2	136.1	21.9
1988.12	345.9	65.2	136.1	21.9
1989.08	14.1	65.2	119.7	7.1
1989.12	14.1	65.2	119.7	7.1
1990.07	17.8	71.1	131.5	7.9
1991.07	17.8	71.1	131.5	7.9
1992.07	17.8	71.1	131.5	7.9
1993.11	**17.8**	**71.1**	**131.5**	**7.9**
1994.10	316.4	64.8	129.2	25.1
1994.11	360	60	129.4	22.1
1994.12	360	60	129.4	22.1

The obtained result coincides with the determination of the fault plane, performed in work (Arefiev and Delui 1998) on the basis of the analysis of aftershock sequences in the area near the source zone of this earthquake. We think that there is a curvature of the contact zone between the oceanic and continental plates at this area and it caused this type of destruction. As a consequence of the above analysis, the choice of the actual fault plane is associated with a greater efficiency of discharging the accumulated internal energy.

Another example of using the criterion (35) is the analysis of sub sources of the Spitak earthquake of 7th December, 1988 (M = 6.9—according to the Richter scale). Table 2 shows the parameters of sub-sources and the main shock (F). The mechanism at the focus of the earthquake was different from the double couple and it had a coefficient of the form of the centroid moment tensor of 0.33. Figure 15 shows: a—the best approximation of the CMT solution; b—the mechanisms of the sub-sources (Arefiev 2003).

The results of the reconstruction allowed us to determine the orientation of the principle stress axes of the stress tensor for the study region: the azimuth and the dip angle of the principal stress—σ_1: 252° and 6°, убрать—σ_3: 157° и 37°, and the Lode-Nadai coefficient $\mu_\sigma \approx 0.3$. The mechanisms of sub-sources were analyzed for the purpose of selecting the actual fault in accordance with the presented approach here. The results of the analysis with the value of the coefficient of the surface friction are shown in table.

Table 2 Parameters of the sub-sources of the Spitak earthquake (Arefiev 2003)

#	Strike	Dip	Slip	$M_{o,}$ 10^{18} Nm
F	290	53	118	0.3
1	295	53	118	4.9
2	322	85	150	3.0
3	300	53	115	1.0
4	305	90	175	1.6
5	305	68	115	2.2

Table 3 The reduced stresses and the criterion (35) for the sub-sources

i	σ^i_{nn}	σ^i_{ss}	$\tilde{\tau}^i_n$	$\tilde{\tau}^i_s$	Criterion (35)
F	−0.260	0.270	0.948	0.180	0.46
1	−0.261	0.277	0.962	0.182	0.39
2	0.828	0.182	0.522	0.520	0.15
3	−0.263	0.281	0.960	0.183	0.45
4	0.503	0.059	0.760	0.870	0.15
5	0.217	0.296	0.971	0.111	0.79

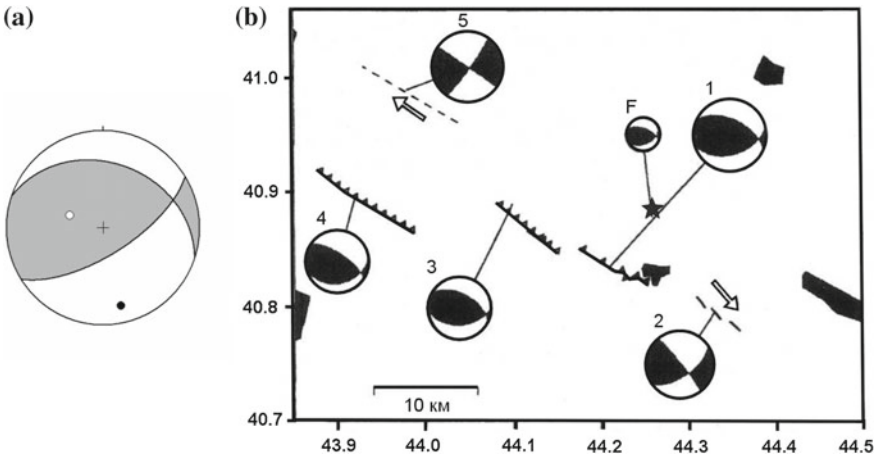

Fig. 15 The earthquake focal mechanism of the Spitak's earthquake (**a**) and a fault map with corresponding earthquake focal mechanisms of the Spitak sub-sources (**b**) (Arefiev, 2003). The asterisk is the epicenter of the main shock

Figure 16 shows the results of the analysis of the actual fault planes of the sub-sources on Mohr diagram in the form of reduced stresses. All the planes that were identified as actual fault planes (on the basis of the analysis of aftershock sequences (Arefiev 2003) satisfy the criterion (35). It can be seen (Fig. 16) that the vectors of reduced stresses determine the position of the points near the largest Mohr circle, and all auxiliary planes (exception is # 4) are located near the central part of the Mohr

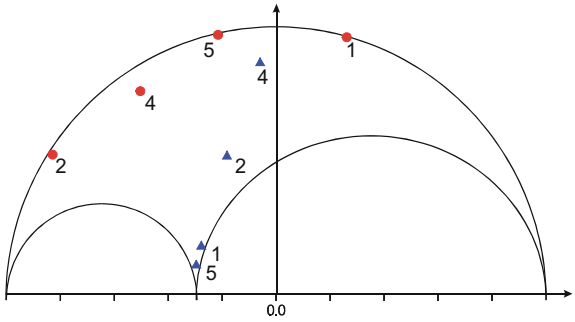

Fig. 16 Analysis of the actual fault planes of the sub-sources of the Spitak's earthquake on the Mohr diagram. Circles—points for nodal planes that satisfy the criterion (35); triangles—points for nodal planes that do not satisfy criterion (35). Point F and point 3 (Table 3) coincide with point 1

diagram, thus that determines the impossibility of realization of these planes for the analyzed stress field.

6 Stress Calculation and Estimation of the Rock Massive Strength Parameters. Third and Fourth Stages of MCA

As noted above, it is possible to obtain only four of the six independent parameters that determine the symmetric stress tensor as a result of the first stage of reconstruction. The relative values of the maximum shear stresses τ/τ_f and the effective pressure p^*/τ_f are determined after the second stage of the reconstruction. The methods for estimating stress values and *strength parameters* of the geo environment will be presented in this paragraph (the third stage of MCA). Stress drop values of the largest earthquakes and the law of conservation of momentum of the force in the vertical direction will be used as additional equations for implementation of the algorithms.

6.1 Determination of the Average Cohesion of the Rock Massive

6.1.1 Algorithm for Estimating the Stress Values on the Basis of Stress Drop Values of the Largest Earthquakes

There are earthquakes with wide range of magnitudes in the region where tectonic stresses are reconstructed. The most effective range of magnitudes for stress reconstruction is the range in which earthquakes with the largest and the low magnitudes are excluded according to the practice of applying the MCA algorithm and the STRESSseism program. The best range is that, for which the difference between the magnitudes is 2–3 units. In the case, when there are many earthquakes with low

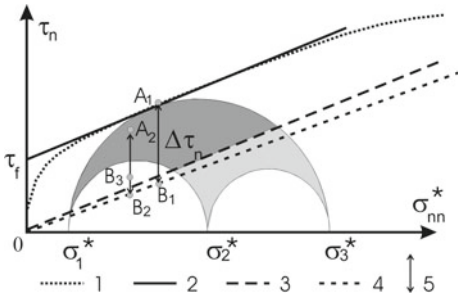

Fig. 17 Geometric analysis of the stress drop on the Mohr's diagram 1—a possible view of the maximum curvilinear envelope, which characterize the limit of the effective internal strength for a rock massif of an average scale that correspond to the scale of the stress parameters reconstructed with the help of MCA; 2—linear approximation of the limiting curvilinear envelope, used in the MCA; 3—line of static friction of rocks; 4—line of kinematic friction of rocks; Area of dark gray color—the geometrical place of points for stresses on the plane of cracks, which can be activated for a given stress tensor (light gray fill—other stress states on arbitrarily oriented planes); 5—the value of the drop of shear stresses points A_1 and A_2

magnitudes the additional stress inversion can be done for these earthquakes, but the difference between the low magnitudes also should be 2–3 units in the range.

Thus, there are some earthquakes which were not used in the reconstruction. The source size of these earthquakes is much more than the source size of those which were used in the reconstruction. Within the framework of the MCA, it is proposed to use such earthquakes to estimate the absolute values of the stresses. The availability of data on the values of shear stresses relieved in the earthquake source for such earthquakes is a necessary condition for the application of the algorithm. These data are the result of the analysis of seismic records based on a complex of seismological methods. Therefore in the MCA, they can be considered as additional. These data form the basis of the third stage of the reconstruction of the stress tensor parameters. It should be noted that, the data on shear stresses relieved in the source area of strong California earthquake were used to estimate the tectonic stress values in the work (Hardebeck and Hauksson 2001).

Such approach became possible, because the MCA allows us to estimate the relative values of the stress drop of the largest earthquakes after the first two stages of reconstruction of the stress parameters. The characteristic linear source dimension of these earthquakes is not less than the characteristic linear dimension of the averaging window for the reconstructed stress tensor parameters. The algorithm for this estimation is illustrated in Fig. 17. This figure shows the vertical segment connecting the point of contact of the limiting envelope with the largest Mohr circle of the state of stress in the area which includes the earthquake source and a line of kinematic friction. The length of this segment (A_1B_1) is equal to the value of the difference of shear stress before and after the earthquake, i.e. ($\Delta\tau_n = \left|\tau_n^0 - \tau_n^1\right|$), for the case when the slip direction coincides with the shear stress direction, which was here before the earthquake.

The possibility of such a geometric interpretation is based on the fact that follows from the theory of destruction (Rice 1980; Osokina 1988): the normal stresses on a fault plane (shear type fracture) remain unchanged before and after fault activation ($\sigma_{nn}^0 = \sigma_{nn}^1 = \sigma_{nn} \leq 0$), as well as shear stresses on the fault (after fault activation) are equal to the value of kinematic friction ($\tau_n^1 = -k_k \sigma_{nn}^*$). The expression for the stress drop value normalized by τ_f can be written in the following form:

$$\begin{aligned} \left\langle \Delta\tau_n/\tau_f \right\rangle &= \bar{\tau}_n \left\langle \tau/\tau_f \right\rangle + k_k \left(\bar{\sigma}_n \left\langle \tau/\tau_f \right\rangle - \left\langle p^*/\tau_f \right\rangle \right) \text{ where} \\ \bar{\tau}_n &= (1-\mu_\sigma)\,\ell_{1n}\ell_{1s} - (1+\mu_\sigma)\,\ell_{3n}\ell_{3s} > 0, \\ \bar{\sigma}_n &= (1-\mu_\sigma)\,\ell_{1n}^2 - (1+\mu_\sigma)\,\ell_{3n}^2 + 2\mu_\sigma/3 < 0. \end{aligned} \tag{35}$$

Here $\bar{\tau}_n$, $\bar{\sigma}_n$—the reduced deviatoric stresses on the fault plane, ℓ_{in}—the direction cosines of the normal to the fault plane of the analyzed earthquake with the principal stress axes σ_i ($i = 1, 3$), and k_k—the coefficient of kinematic friction.

The stresses normalized by τ_f are marked with angle brackets in expression (35), as it was done in the previous paragraph. Thus, the right-hand side of the expression (35) is completely defined after the first ($\bar{\tau}_n$, $\bar{\sigma}_n$) and second ($\left\langle \tau/\tau_f \right\rangle$,$\left\langle p^*/\tau_f \right\rangle$) stages of the reconstruction.

In the MCA algorithm, implemented in calculations below, the value of static friction k_s and effective internal friction k_f were assumed at 0.6, and the value of kinematical friction k_k was 0.5. The possibility of using expression (35) implies the constancy of fluid pressure in each of the calculated domains at the moment of rupture activation ($p_{fl}^0 = p_{fl}^1$). The first summand in (35) characterizes the values of shear stresses, acting along the fault plane before the earthquake (point A_1 in Fig. 17), and the second one does the shear stresses τ_n^1, which will act here after the earthquake (point B_1 in Fig. 17).

After the calculation of the relative value $\left\langle \Delta\tau_n/\tau_f \right\rangle$ by the data of the first two stages of MCA, we might estimate τ_f. As additional data, we use the value of stresses $\Delta\tau_n$ discharged during the large earthquake:

$$\tau_f = \frac{\Delta\tau_n}{\left\langle \Delta\tau_n/\tau_f \right\rangle}. \tag{36}$$

The value $\Delta\tau_n$ on the right of (36) is defined with the use of data on the scalar value of seismic moment M_o and from the earthquake source geometry (Kasahara 1981):

$$\Delta\tau_n = \chi M_o/(WL^2), \tag{37}$$

where L and W are the length (the greatest of the subhorizontal dimensions) and the width of the earthquake source, and χ is a parameter dependent on the type of displacement in the earthquake source (normal fault, revers, or strike-slip fault) and on its geometrical form ($0.65 \leq \chi \leq 1.85$).

It is shown in (Kostrov 1975; Kostrov and Das 1988) that if the energy associated with change in the area of the growing rupture surface is negligible and we consider that shear stresses after the beginning of displacement along the rupture have not changed, but remained equal to the kinematic friction, then shear stresses discharged in the earthquake source could be defined using the data on released seismic energy E_s:

$$\Delta\tau_n = 2\mu E_s / M_o, \tag{38}$$

where μ is the shear elastic modulus (for the crust $\mu \approx 3$–$5\ 10^4$ MPa), E_s and M_o are presented in joules.

It should be noted there that there is a proportion in seismology that allows us to estimate the socalled apparent stresses $\bar{\tau}_n = \left|\tau_n^0 + \tau_n^1\right|/2$, which is the average stress between the two states at the rupture, on the basis of data on seismic energy:

$$\eta\bar{\tau}_n = \mu E_s / M_o, \tag{39}$$

where $\eta = \Delta\tau_n / 2\bar{\tau}_n$ (Kostrov 1975; Kostrov and Das 1988) is the so called seismic efficiency. Expression (39) is often used for definition of $\bar{\tau}_n$. But, due to the great uncertainty of the η value, such estimations cannot consider reliable.

The value E_s in expression (39) could be obtained using correlation dependences with the magnitude of earthquake M_e, which characterizes energy radiated in seismic waves:

$$\log\ E_s = 3M_e/2 + 4.35. \tag{40}$$

If the destruction is implemented along the previously existing rupture, which has not restore its cohesive strength to the undistracted state ($\tau_s < \tau_f$), then on the Mohr diagram the vertical segment, which characterizes stress drops, begins from the point lying below the limit envelope, but higher than the line of minimum resistance due to dry static friction (the segment A_2B_2 in Fig. 17). In the case when the slip direction along the rupture does not coincide with the shear stress direction acting on the plane before activation, the vertical segment does not reach the line of resistance due to kinematic friction (the segment A_2B_3 in Fig. 17).

The stress parameters substituted into expression (35) should correspond the averaging period, which precedes the strong earthquake, and data on its stress drop will be used for determining τ_f. For example, using the catalogue of earthquake focal mechanisms with the range of magnitudes of 4.5–7 allows us to tell that the reconstructed parameters of the stress tensor may correspond to the averaging scale of 20–100 km. The exact value depends on the density of the distribution of earthquake foci, and the range of magnitudes of 2.5–6 may correspond to the averaging scale of 5–30 km. In this case strong earthquakes, whose stress drop can be used for estimation of internal cohesion, should not have magnitudes less than 6.5 and 5.5 correspondingly, i.e., the focal area should not be less than the stress averaging window. The algorithm of the third stage of MCA allows us to estimate the value of effective internal cohesion of

rock τ_f, and then, using the data on relative values of maximum shearing stress and effective pressure (the second stage of MCA), transit to their absolute values.

$$\tau = \left\langle \frac{\tau}{\tau_f} \right\rangle \tau_f, \quad p^* = \left\langle \frac{p^*}{\tau_f} \right\rangle \tau_f. \tag{41}$$

It should be noted that the deviatoric component of the stress tensor is defined after the third stage of the MCA, but the spherical component of the stress tensor is not defined. The effective pressure p^* includes two unknown values - isotropic tectonic pressure and fluid pressure in the fractured-pore space.

6.1.2 Examples of Estimation of the Value of Effective Internal Cohesion of Rock Massif

For calculation of τ_f, we will use the data on values of the stress drops of the Simushir earthquake November 15, 2006 ($M_w = 8.3$). The stresses acting in the crust of the northwestern flank of the Pacific seismoactive area before the Simushir earthquake was implemented on a 3D grid for the layer with the median surface at a depth of 20 km. The grid step was 0.2° on the basis of earthquake focal mechanisms data of Global CMT Project. The most representative range of earthquake magnitudes from this catalogue for the studied part of the crust is $5.5 > M_w > 6.5$, and the distribution density of their foci allowed us to tell about the averaging scale of stress parameters of 50–70 km.

To estimate τ_f, the seismological data on energy parameters of the Simushir earthquake event were used. The value of energy released in seismic waves E_s and the seismic moment M_o of the Simushir earthquake were correspondingly 7.4×10^{16} and 3.4×10^{21} J, according to the data of Global CMT Project. The fault parameters of the Simushir earthquake, according to the CMT Project, were the following: Strike1 = 215°, Dip1 = 15°; Strike2 = 33°, Dip2 = 75° (thrust faulting).

The results of seismic inversion (http://earthquake.usgs.gov/eqcenter/eqachives/poster/2006/20061115_image.php) show that the actual fault plane was the first nodal plane, This plane corresponded to the gentle dipping (15°) of the subducted oceanic plate under the subcontinental plate and had a length along the Trench (W) of about 400 km, while in the cross direction (L) of about 130 km (solid line contour in Fig. 18). The analysis of distribution of the aftershock sequences, made in (Tikhonov et al. 2007), gives correspondingly 300 and 60 km (thin line contour in Fig. 18).

Using the data on energy released during the Simushir earthquake, through expression (38) we find $\Delta\tau_n \approx 1.7$ MPa (17 bar). If we use expression (37) and data on the earthquake source geometry (with $\chi = 1$, because the earthquake source area is not isometric), then we will obtain $\Delta\tau_n \approx 0.5$ MPa (by the Global CMT Project data), $\Delta\tau_n \approx 1.4$ MPa (by works Tikhonov et al. 2007). The presented results show that calculation of $\Delta\tau_n$ by the CMT Project data on the earthquake source dementions understates the value, while the estimation of source geometry in the work (Tikhonov et al. 2007) gives a better correspondence to the energergy parameters of the earth-

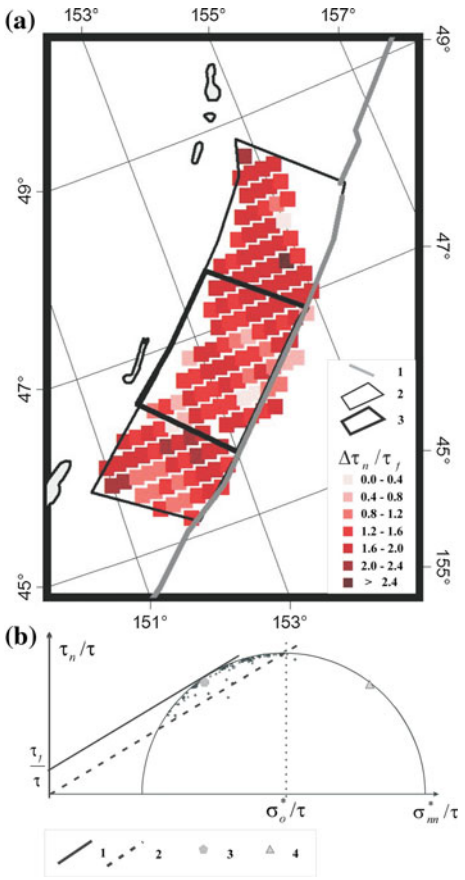

Fig. 18 **a** Distribution of the values of shear stresses normalized by τ_f for Simushir earthquake calculated within the framework of the third stage algorithm of the MCA. 1—oceanic Trench, 2—geometry of the used in our calculation (Tikhonov et al. 2007), 3—geometry of the Simushir earthquake source by the Global CMT Project data. **b** For the generalizing Mohr diagram, there is the position of points with values of the normalized normal and shear stresses along the source areas of these earthquakes. Normalization is made by the value of maximum shear stresses corresponding to the domain with parameters of the stress tensor, which is the closest to the beginning of earthquake rupture. Here the solid line is the limit of effective strength (1); the dashed line is the line of minimum dry friction (2); the pentagon (3) and triangle (4) with light gray fill correspond to the stresses along the fault and auxiliary nodal planes of focal mechanisms Simushir earthquake

quake. In the following calculations, we will use the source geometry given in these works. The value of stress drop in the source area of Simushir earthquake can be obtained, with a precision to valuation at the unknown value of effective adhesion of rock massif τ_f, using the results of the first two stages of MCA reconstruction and expression (35). For the source area of Simushir earthquake, 90 domains exist for which the data on stress tensor parameters were obtained (Fig. 18).

Using the data of these domains and summing the contribution in stress drop for the parts of the earthquake source within each domain, on the basis of expression (35) and data on the earthquake source dementions, we find the average value of ratio $\langle \Delta\tau_n/\tau_f \rangle = 1.41$. Next, using the data on values of the stress drop, we find the value of effective cohesion $\tau_f = 1.0 - 1.2$ MPa.

6.2 *Estimation of the Isotropic Pressure Using the Equations of Equilibrium of Shallow Shells*

6.2.1 Defining Equations of the Theory of Shallow Shells and Thick Plates

The results of the three stages of reconstruction by the MCA algorithm make it possible to determine all the stress tensor components (the principal stresses are reduced ($\sigma_i^*, i = 1, 2, 3$) by the level of the fluid pressure). Thus, the tectonic pressure p and the fluid pressure p^* remain unknown, and effective pressure p^* is the difference between these two values. To determine them, it is proposed to use the fact that the stress data obtained for discrete grid nodes of the geo-medium must satisfy the notion of the stress field.

The notion of stress field in mechanics is understood as the continuity of the stress components, which requires them to satisfy the differential equations of conservation of the momentum of the force. Violation of this requirement is possible at the contact boundaries of essentially different properties of the mediums and at the fault boundaries in the case of a displacement jump.

According to the results of the natural stress inversion, as a rule, data on stresses are obtained in averaging scale comparable to the thickness of the crust or its main layers. Therefore, the equation of the law of momentum conservation of forces, or the equation of equilibrium, can be written in a simplified form, used in the theory of shallow shells and thick plates (Timoshenko and Goodier 1970):

$$\begin{aligned}
&\frac{\partial \widehat{\sigma}_{xx}}{\partial x} + \frac{\partial \widehat{\sigma}_{xy}}{\partial y} + \frac{T_{xz}^{\xi} - T_{xz}^{\varsigma}}{h} = 0,\\
&\frac{\partial \widehat{\sigma}_{xy}}{\partial x} + \frac{\partial \widehat{\sigma}_{yy}}{\partial y} + \frac{T_{yz}^{\xi} - T_{yz}^{\varsigma}}{h} = 0,\\
&\frac{\partial \widehat{\sigma}_{xz}}{\partial x} + \frac{\partial \widehat{\sigma}_{yz}}{\partial y} + (\kappa_{xx}\widehat{\sigma}_{xx} + \kappa_{yy}\widehat{\sigma}_{yy}) + \frac{N_{zz}^{\xi} - N_{zz}^{\varsigma}}{h} + \widehat{\gamma} = 0,
\end{aligned} \tag{42}$$

where z—a vertical axis directed toward the center of the earth, $h(x, y) = \xi(x, y) - \zeta(x, y)$—thickness of the layer, changing laterally and estimated taking into account the irregularities of the surface of its roof ζ and bottom ξ, κ_{xx} and κ_{yy}—the curvature

of the shell in the proper directions, $\widehat{\gamma}(x, y)$—the average specific weight of the rocks of the upper crust, is equal to

$$\widehat{\gamma} = \frac{1}{h} \int\limits_{\zeta(x,y)}^{\xi(x,y)} \gamma(x, y, z) dz, \tag{43}$$

$\widehat{\sigma}_{ij}$—the average stresses are defined as:

$$\widehat{\sigma}_{ij} = \frac{1}{h} \int\limits_{\zeta(x,y)}^{\xi(x,y)} \sigma_{ij} dz, i, j = x, y, z, \tag{44}$$

and $T_{xz}^{\xi} = \sigma_{xz}|^{\xi}$, $T_{yz}^{\xi} = \sigma_{yz}\big|^{\xi}$, $N_{zz}^{\xi} = \sigma_{zz}|^{\xi}$ и $T_{xz}^{\varsigma} = \sigma_{xz}|^{\varsigma}$, $T_{yz}^{\varsigma} = \sigma_{yz}\big|^{\varsigma}$, $N_{zz}^{\varsigma} = \sigma_{zz}|^{\varsigma}$—the stresses applied to the bottom and roof of the layer under consideration. It should be noted that when equations were written in the form (42), the condition of absence of the loading on the daylight surface of the earth's crust is used. An approximate representation of the equilibrium equations in the form (42) is valid for a slow change along the lateral thickness of the layer.

We shall accept the linear distribution law along the z axis for the normal and shear stresses acting on the horizontal planes. In this case, the average stress in the layer can be related to the stresses acting along its roof and the bottom by simple expressions:

$$\widehat{\sigma}_{xz} = 0.5\left(T_{xz}^{\zeta} + T_{xz}^{\xi}\right), \ \widehat{\sigma}_{yz} = 0.5\left(T_{yz}^{\zeta} + T_{yz}^{\xi}\right), \ \widehat{\sigma}_{zz} = 0.5\left(N_{zz}^{\zeta} + N_{zz}^{\xi}\right). \tag{45}$$

Further, we will put a tilde over the stress tensor parameters, realizing that these stress tensor parameters determine the average value of the stresses. These average stresses (in the accepted linear approximation of the peculiarities of distribution of the stresses in depth) can be regarded as stresses which related to the middle surface of the layer (shell). We shall also neglect the sphericity of the Earth's surface, assuming in the last expression of the set of equations (42), that $\kappa_{xx} = 0$, $\kappa_{yy} = 0$, writing the equilibrium equations, going from the theory of shallow shells to the theory of thick plates.

6.2.2 Calculation of the Value of the Confining Pressure *p*

Calculation of stresses in a layered shell should be carried out sequentially from the upper layer to the lower layers. This is due to the fact that on the roof of the upper layer of the shell (see Fig. 19) the normal and shear stresses are zero and, consequently, here

$$\widehat{\sigma}_{xz} = 0.5T_{xz}^{\xi}, \ \widehat{\sigma}_{yz} = 0.5T_{yz}^{\xi}, \ \widehat{\sigma}_{zz} = 0.5N_{zz}^{\xi}. \tag{46}$$

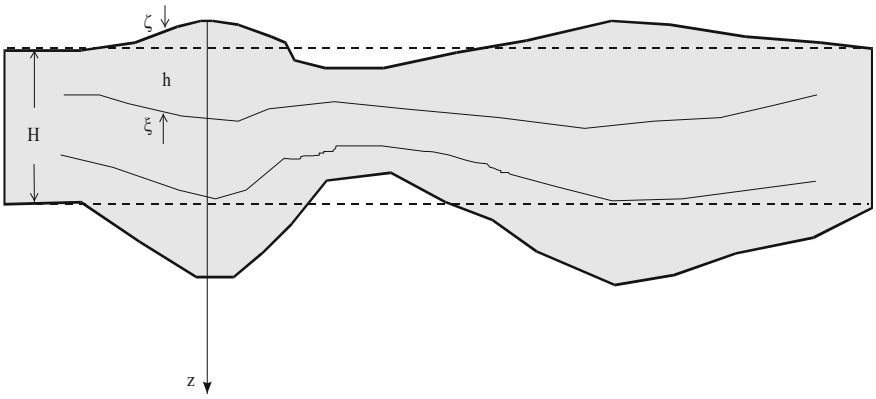

Fig. 19 Approximation scheme of layers of the earth's crust by shallow shells, H—the average thickness of the earth's crust

Using the expressions (31), (32), we will replace the stresses σ_{ij} in the expressions (42), through the reduced stresses $\tilde{\sigma}_{ij}$ and values p, τ,

$$
\begin{aligned}
&-\frac{\partial p}{\partial x}+\widehat{\sigma}_{xx}\frac{\partial \tau}{\partial x}+\widehat{\sigma}_{xy}\frac{\partial \tau}{\partial y}+\left(\frac{\partial \widehat{\sigma}_{xx}}{\partial x}+\frac{\partial \widehat{\sigma}_{xy}}{\partial y}+\frac{2\widehat{\sigma}_{xz}}{h}\right)\tau=0,\\
&-\frac{\partial p}{\partial y}+\widehat{\sigma}_{xy}\frac{\partial \tau}{\partial x}+\widehat{\sigma}_{yy}\frac{\partial \tau}{\partial y}+\left(\frac{\partial \widehat{\sigma}_{xy}}{\partial x}+\frac{\partial \widehat{\sigma}_{yy}}{\partial y}+\frac{2\widehat{\sigma}_{yz}}{h}\right)\tau=0,\\
&-\frac{2p}{h}+\widehat{\sigma}_{xz}\frac{\partial \tau}{\partial x}+\widehat{\sigma}_{yz}\frac{\partial \tau}{\partial y}+\left(\frac{\partial \widehat{\sigma}_{xz}}{\partial x}+\frac{\partial \widehat{\sigma}_{yz}}{\partial y}+\frac{2\widehat{\sigma}_{zz}}{h}\right)\tau+\widehat{\gamma}=0.
\end{aligned}
\tag{47}
$$

It should be reminded that the reduced values of the stresses are determined by the values of the direction cosines of the angles of the principle stresses with the coordinate axes $j = x, y, z$ (ℓ_{ij}) and the Lode-Nadai coefficient (μ_σ) and they are calculated from the results of the first stage of the reconstruction. The parameters of the unknown stress tensor refer to the middle of the shell layer.

The set of equation (47) can be written in an orthogonal curvilinear coordinate system: one coordinates is vertical, and the other two are in the horizontal plane. We will consider that one of the coordinate directions coinciding with the shear stress acting on the horizontal planes (Fig. 20). We will define these stresses as underthrusting shear stresses, i.e. they are responsible for under-thrust faults. The last equation in the (47) can be written in the form, using such a representation of the law of momentum conservation in the vertical direction:

$$
p=\widehat{\gamma}\frac{h}{2}+\tau\widehat{\sigma}_{zz}+\frac{h}{2}\frac{\partial}{\partial s}\left(\widehat{\sigma}_{sz}\tau\right). \tag{48}
$$

where s—coordinate along the shear stresses acting on horizontal planes (see Fig. 20).

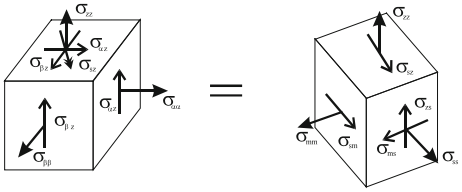

Fig. 20 The loading scheme of a parallelepiped, connected with the direction of the shear stress on the middle surface of the shell

It should be pointed out that the expression (48) is more accurate than the calculation of tectonic pressure on the basis of R. Sibson hypothesis (Sibson 1974) in which the vertical stresses acting on horizontal planes are equated with the pressure exerted by the weight of the overlying rocks. It should be noted that the Sibson's condition can be obtained from (48) by putting $\widehat{\sigma}_{sz} = 0$.

The value of the isotropic pressure of the investigated area of the earth's crust can be estimated using the data on the relative value of the maximum shear stress obtained after the second stage of the MCA, data on the s direction for underthrusting shear stresses on the horizontal plane (the first stage of the MCA), and also assuming the values of the maximum shear stresses (the third stage of the MCA). After that, the value of the fluid pressure (it is average for the scale of the obtained stress data) can be determined:

$$p_{fl} = p - p^*. \tag{49}$$

Note that one of the other two equations of conservation of momentum in the horizontal direction can be used to verify the accuracy of estimation of stresses during the first three stages of reconstruction, rewriting it in the s direction:

$$\left(-p + \widehat{\sigma}_{xx}\tau\right)_{s_1} = \left(-p + \widehat{\sigma}_{xx}\tau\right)_{s_0} - \frac{2}{h}\left(\tau\widehat{\sigma}_{xz}\right)_{s_0}. \tag{50}$$

Here the subscripts are behind the brackets: s_0 and s_1 are two consecutive coordinates of the points along the s trajectory for which verification is performed.

7 Conclusion

Some theoretical principles of geomechanics and tectonophysics were presented in this work. These principles are subject to the problem of creating a methodology for studying the stress-strain state and the mechanical properties of rock massif. It is important to note that the developing approach is based on the difference in solid samples and natural massifs, (which have a multitude of defects in the form of low strength surfaces), deformation behavior. The developed methodological principles for reconstructing the parameters of tectonic stresses and increments for seismotectonic deformations can be considered as a tool, which uses for this purpose active

tectonic faults and fractures. It can be said that the creation of methods for studying the natural stresses in the rock massif is equivalent to the laboratory tools: (a dynamometer and a ruler, which are used by experimenter in laboratory modeling). At the same time, the scale of the solid samples and natural massifs are incommensurable.

The basis of the algorithm of calculation of the stress-strain state parameters is composed of approaches, following from a number of fundamental principles of the continuum mechanics and mechanics of rupture destruction. These approaches allowed the formulation of energetic criteria, defining the concepts of generalized stresses responsible for the activation of old faults and creation of new ones, and released generalized deformations, formed in geo-environment results of faulting displacements. The totality of these criteria characterizes the stage of the steady-state quasi-plastic f1owing, during which loading conditions and stresses, acting in natural massifs, remain stable at rather long time intervals in the process of deformation. This stage is characterized by the associated flow law. The energetic criteria determine the requirements for the dissipation of internal energy on the discontinuous displacements and the monotonic elasto-plastic deformation, which is a consequence from the Von Mises's maximum principle. Energetic criteria composed the basis of the method of cataclastic analysis and allowed formalization of the principles of creation of homogeneous samplings of structural-kinematic data on slip faults (earthquake source mechanisms).

In the framework of the MCA, it was possible to show that a number of well-known methods of stress inversion (defining inequalities of the kinematic method by Gushchenko (Goustchenko 1996) and the right dihedral method by J. Angelier (Angelier and Mechler 1977)) directly follow from the condition of a decreasing internal energy after discontinuous displacements. This fact made it possible to revise one of the main principles of the Batdorf-Budyansky's dislocation theory of plasticity (Batdorf and Budiansky 1949), about the coincidence of the slip direction and the shear stresses (acting before the fault), which was used in a number of methods for reconstruction of the tectonic stresses. It is established that the faults of identical hierarchical level influence on each other. Displacements for simultaneously activated and closely located faults, are determined not only by the initial stress field, but also by the fault configuration. Analysis of displacements in the source areas of the largest earthquakes showed that they form the tensor of the released deformations, which is maximally approximated (in the form and orientation of the principle axes) to the stress tensor that was before the earthquake. It is in this case, the most effective internal energy dissipation in the vicinity of the earthquake source area is achieved.

Theoretical analysis of the properties and peculiarities of quasi-plastic flow, developing under the action of loading in fractured media, have shown, that its character changes depending on the intensity of deviatoric components of the stress tensor and on the value of the effective pressure (accounting for the fluid pressure). The earlier stage of fracturing deformation, during which new ruptures or faults are not formed, is resulted from the activation of the existing fault structure and is characterized by the non-associated flowing law, whereas, at the stage of the maximum effectiveness

of quasi-plastic deformation, the flowing law tends to become the associated one. These peculiarities lead to the fact that, at the initial stage of quasi-plastic flowing, only a part of energetic criteria of the method of cataclastic analysis hold (criterion of internal energy dissipation on rupture displacements). The fulfillment of all these criteria of the method of cataclastic analysis takes place at the limiting stage, for which in natural massifs, along with activation of pre-existing faults, new ruptures are also formed.

A certain dual nature of the discontinuous deformations, (which on the one hand, represent an act of destruction, and on the other hand, characterize the deformation properties of the continuum), predetermines sequence of the reconstruction stages of the stress-strain state parameters. In the MCA, during the first stage: the energy principles of the continuum mechanics are used, the formation of homogeneous SKD samples is performed, the parameters characterizing the ellipsoids of the stress tensor and quasiplastic deformations are calculated: the orientation of the main semi-axes (principle stresses and increments for seismotectonic deformations) and their ratio (Lode-Nadai coefficient). During the second stage: these stress parameters and the formed homogeneous samples are the basis for determining the relative stress values. Here, the principles of the mechanics of destruction that define the natural massifs as an initially fractured Coulomb medium are used.

It is important to note that formulation of the conditions of fracturing of natural massif (creation of new faults and activation of previously existed ones) is accepted in the Method of Cataclastic Analysis in its general form, satisfying the results of experiments on rock sample fracturing. Defining parameters of Coulomb's condition were considered as unknown. The determination of these strength parameters and the stress values is performed during the third stage of the MCA. The principles of the continuum mechanics are again used, in particular, the law of momentum conservation in the vertical direction, written in the approximation of shallow shells.

The homogeneous samples set of SKD are the most important element of the investigations. They are formed as the results of the first stage of reconstruction based on the energetic criteria. In fact, it is the homogeneous samples set of SKD made it possible to make a qualitative jump from the determination of the orientation of the principal axes of the stress tensors and increments for seismotectonic deformations to the calculation of the value of the spherical and the intensity of the deviatoric components of these tensors. It can also be drawn an analogy with laboratory experiments in which in order to estimate the strength parameters of brittle rock samples it is necessary to have the measures of the morphological parameters of the forming discontinuous structures, with respect to the loading stresses.

At the second stage of calculations, the key issue for the estimation of modem stresses from data on earthquake source mechanisms is the method of determining the fault plane, suggested in this work. This method is based on the application of the Coulomb's criterion within the frameworks of the limiting state theory for selecting one of the two nodal planes, which is realized as the fault plane in the earthquake source. According to the suggested method, that of the nodal planes is selected, for which the maximum release of the shear stresses is achieved. The effectiveness of such method of selecting the realized plane of source is verified on the strongest

earthquake. The use of the Coulomb failure criterion together with the analysis of earthquakes dynamic data on the Mohr's circle made it possible to develop principles for estimating the rock mass strength parameters, such as the coefficients of static and kinetic friction.

The determination of the stress values is possible with the use of additional equations including seismological data on the dynamic source parameters of the largest earthquakes (shear stress drop) and the law of momentum conservation in the vertical direction. Previously, this type of data has already been used in a number of works on the study of natural stresses (R. Sibson, J Hardebeck).

Currently, the computer programs that allow working with both seismological (STRESSseism) and geological (STRESSgeol) data on discontinuous displacements have been created on the basis of the MCA algorithm. The performed reconstruction of the modern state of stress for the intracontinental orogens regions (Rebetsky et al. 2012) and active continental margins (Rebetsky and Tattevossian 2013) allow us to identify a number of important regularities.

References

Angelier J (1975) Sur l'analyse de measures recueilles dans des sites failles: l'utilite d'une confrontation entre les methods dynamiques et cinematiquues. Bull Soc Geol France 281:1805–1808

Angelier J (1984) Tectonic analysis of fault slip data sets. Geophys Res 89(B7):5835–5848

Angelier J, Mechler P (1977) Sur une methode graphique de recherche des contraintes principales egalement utilisable en tectonique et en seismologie: la methode des diedres droits. Bull Soc Geol Fr V XIX 6:1309–1318

Arefiev SS, Delui B (1998) The focal zone of the Shikotan earthquake of 1994: the choice of the active plane. Phys Earth 6:64–74

Arefiev SS (2003) Epicentral seismological studies. Moscow, Akademkniga. p 374 (in Russian)

Batdorf SB, Budiansky B (1949) A mathematical theory of plasticity based on the concept of slip. NASA Technical Note 1871

Bott MHP (1959) The mechanics of oblique slip faulting. Geol Mag 96:109–117

Bridgman W (1949) Studies in large plastic flow and fracture, with special emphasis on the effects of hydrostatic pressure. McGraw-Hill Book Co., Inc., New York, p 362

Byerlee JD (1967) Frictional characteristics of granite under high confining pressure. J Geophys Res 72(14):3639–3648

Byerlee JD (1978) Friction of rocks. Pure Appl Geophys 116:615–626

Byerlee JD (1968) Brittle-ductile transition in rocks. J Geophys Res 73(14):4741–4750

Carey E, Bruneier B (1974) Analyse theorique et numerique d'un modele mecanique elementaire applique a l'etude d'une populaton de failles. C R Acad Sci Paris D 279:891–894

Chernykh KF (1998) An introduction to modern anisotropic elasticity. Begell Publishing House, New York, p 282

Dobrovol'sky IP (2009) Mathematical theory of preparation and prediction of earthquakes. FIZMATLIT. Moscow, p 240 (in Russian)

Drucker DC (1959) A definition of stable inelastic material. Trans ASME, J Appl Mech 101–106

Goustchenko OI (1975) Kinematic principle of reconstruction of directions of main stresses (on geological and seismological data) DAN USSR Ser Geophys 225 (3):557–560 (in Russian)

Goustchenko OI (1996) Seismotectonic stress-monitoring of the lithosphere (structural-kinematic principle and basic elements of the algorithm) DAN USSR Ser Geophys 346 (3):399–402 (in Russian)

Handin J (1969) On the Colombo—Morh failure criterion. J Geophys Res 74(22):5343–5348
Hardebeck JL, Hauksson E (2001) Crustal stress field in southern California and its implications for fault mechanics. J Geophys Res 106(B10):21859–21882
Kasahara K (1981) Earthguake mechanies. Cambriage University Press, p 284
Knopoff L (1958) Energy release in earthquakes. Geophys J MNRAS 1: 44–52
Kostrov BV (1975) Mechanics of tectonic earthquake source. Nauka Наука, Moscow, p 176 (Russia)
Kostrov BV, Das S (1988) Principles of earthquake source mechanics. In: Cambridge monographs on mechanics and applied mathematics. Cambridge University, Cambridge, New York, Port Chester, Melbourne, Sydney, p 286
McKenzie Dan P (1969) The relation between fault plane solutions for earthquakes and directions of the principal stresses. Bull Seism Soc Am 59(2):591–601
Mises RV (1928) Angew Math Mech 8:161–185
Mogi K (1964) Deformation and fracture of rocks under confining pressure (2) compression test on dry rock sample Bul Earthq Res Inst Univ Tokyo 42(Part 3):491–514
Mogi K (1966) Pressure dependence of rock strength and transition from brittle fracture to ductile flow. Bull Earthq Res Inst Univ Tokyo 44:215–232
Nikolaevskiy VN (1996) Geomechanics and fluidodynamics. Kluwer, Dordrecht, p 349
Osokina DN (1988) Hierarchical properties of a stress field and its relation to fault displacements. J Geodyn 10:331–344
Paul B (1968) Macroscopic criteria for plastic flow and brittle fracture. In: Liebowitz H (ed) Fracture. An advanced treatise, vol 2. Academic Press, New York, pp 313–496
Rebetskii YuL (2003) Development of the method of cataclastic analysis of shear fractures for tectonic stress estimation. Dokl Earth Sci 388(1):72–76
Rebetsky YuL (1999) Methods for reconstructing tectonic stresses and seismotectonic deformations based on the modern theory of plasticity. Dokl Earth Sci 365A(3):370–373
Rebetsky YuL, Lermontova AS (2016) Accounting for the supercritical state of the geoenvironment and the problem of the long-range effect of earthquake foci. Vestnik Kraunts Nauka Zemle 32:115–123 (In Russia)
Rebetsky YuL, Polets AYu, Zlobin TK (2016) The state of stress in the earth's crust along the northwestern flank of the Pacific seismic focal zone before the Tohoku earthquake of 11 March 2011. Tectonophysics 685:60–76. https://doi.org/10.1016/j.tecto.2016.07.016
Rebetsky YuL, Sycheva NA, Kuchay OA, Tatevossian RE (2012) Development of inversion methods on fault slip data: stress state in orogenes of the central Asia. Tectonophysics 581:114–131. https://doi.org/10.1016/j.tecto.2012.09.027
Rebetsky YuL, Tatevossian RE (2013) Rupture propagation in strong earthquake sources and tectonic stress field. Bull Soc Geol Fr 184(4–5):335–346
Rice J (1980) The mechanics of earthquake rupture. In: Dziewonski AM, Boschi E (eds) Physics of the earth's interior. North-Holland, Amsterdam, pp 555–649
Rummel F, Alheid HJ, Frohn C (1978) Dilatancy and fracture induced velocity changes in rock and their relation to friction sliding pure and app. Geophys 116:743–764
Sibson RH (1974) Frictional constraints on thrust, wrench and normal faults. Nature 249:542–544
Starr AT (1928) Slip in crystal and rupture in solid due to shear. Proc Camb Phil Soc 24:489–500
Shteynberg VV (1983) On focal parameters and seismic effect of earthquakes. Izv Academy Sci USSR Phys Earth (7): 536–548
Stesky RM (1978) Rock friction-effect of confining pressure, temperature, and pore pressure Pure App. Geophys 116:691–704
Terzaghi K (1943) Theoretical soil mechanics. Wiley, New York, p 506
Tikhonov IN, Vasilenko NF, Prytkov AS, Spirin AI, Frolov DI (2007) Catastrophic simushir earthquakes November 15, 2006 and January 13, 2007. Probl Seismic sound Far East and East Sib: Intern Sci Simp Yu-Sakhalinsk: Izd IMGG FEB RAS. From 27–28 (Russian)

Timoshenko SP, Goodier JN (1970) Theory of elasticity. McGraw-Hill Book Company, New Yurk, p 576
Wallace RE (1951) Geometry of shearing stress and relation to faulting. J Geol 59:18–130
Wells DL, Coppersmith KJ (1994) New empirical relationship among magnitude, rupture length, rupture width, rupture area, and surface displacement. Bull Seism Soc Am 84(4):974–1002